PRE-DOSE EFFECT AND POSSIBLY-RELATED POINT DEFECTS IN CRYSTALLINE QUARTZ

By

XIAO-HUA YANG

Bachelor of Science

Xinxiang Normal University

Xinxiang, Henan, China

1984

Submitted to the Faculty of the
Graduate College of the
Oklahoma State University
in partial fulfillment of
the requirements for
the Degree of
MASTER OF SCIENCE
December, 1988

PRE-DOSE EFFECT AND POSSIBLY-RELATED POINT DEFECTS IN CRYSTALLINE QUARTZ

Thesis Approved:

Stephen McKeever
Thesis Advisor

Joel J. Martin

Larry E. Halliburton

Norman N. Durham
Dean of the Graduate College

ACKNOWLEDGEMENTS

I would like to express my gratitude to my thesis advisor, Dr. S. W. S. McKeever, for his kind guidance, encouragement, and friendship throughout this project. Without his help, it would be impossible for this thesis to be completed. From him I learned not only the science but also the quality a scientist should have. I would also like to thank Dr. L. E. Halliburton and Dr. J. J. Martin for serving on my thesis committee. Many helpful discussions with them are also greatly appreciated. The kind permission by Dr. L. E. Halliburton to use EPR instruments in his lab is greatly acknowledged.

I would also like to thank Dr. C. Y. Chen, Dr. R. Hantezadeh, and Mr. M. Scripsick for their help and assistance in using the EPR machine. I also wish to thank Mr. D. Hart and Mr. C. Hunt for their help in the use of the facilities in the crystal growth lab.

Most importantly, I wish to thank my family for their love, support, and the encouragement throughout my education. Especially, I would like to thank my wife, Yumei Zhou, for her understanding and for her help of drawing all the figures in this thesis.

Financial support from the National Science Foundation for this project is deeply appreciated.

Finally, I would like to thank Mr. Bin Fang for his great effort in typing this thesis.

TABLE OF CONTENTS

LIST OF FIGURES

CHAPTER I

INTRODUCTION

The "Pre-Dose" Effect

The "Pre-Dose" Effect is a unique characteristic of the thermoluminescence (TL) response of alpha quartz. It concerns the remarkable increase in sensitivity of the 110 °C TL peak in quartz following pre-exposure of the sample to radiation (i.e., the "Pre-Dose") and heating to approximately 500 °C. The fundamental observations of the Pre-Dose Effect can be best explained via figure 1 (1). The quartz sample used has been fired (by firing we mean that the sample has been heated to a high temperature (about 1000 °C) for extended times, (typically 1-2 hours)). After a large Pre-Dose N is given to it, the sample is then heated to beyond 150 °C to remove any TL signal associated with the 110 °C peak. After this pre-treatment, the sample is given a small test dose of 1×10^{-2} Gy and the TL is monitored. This produces a small peak at 110 °C of S_0, taken to be representative of the initial sensitivity of the peak. The sample is then heated to 500 °C before being cooled to room temperature and re-irradiated again with a 1×10^{-2} Gy test dose. Subsequently, this is found to give an enhanced signal of size S_N. A successive heating to 500 °C and 1×10^{-2}

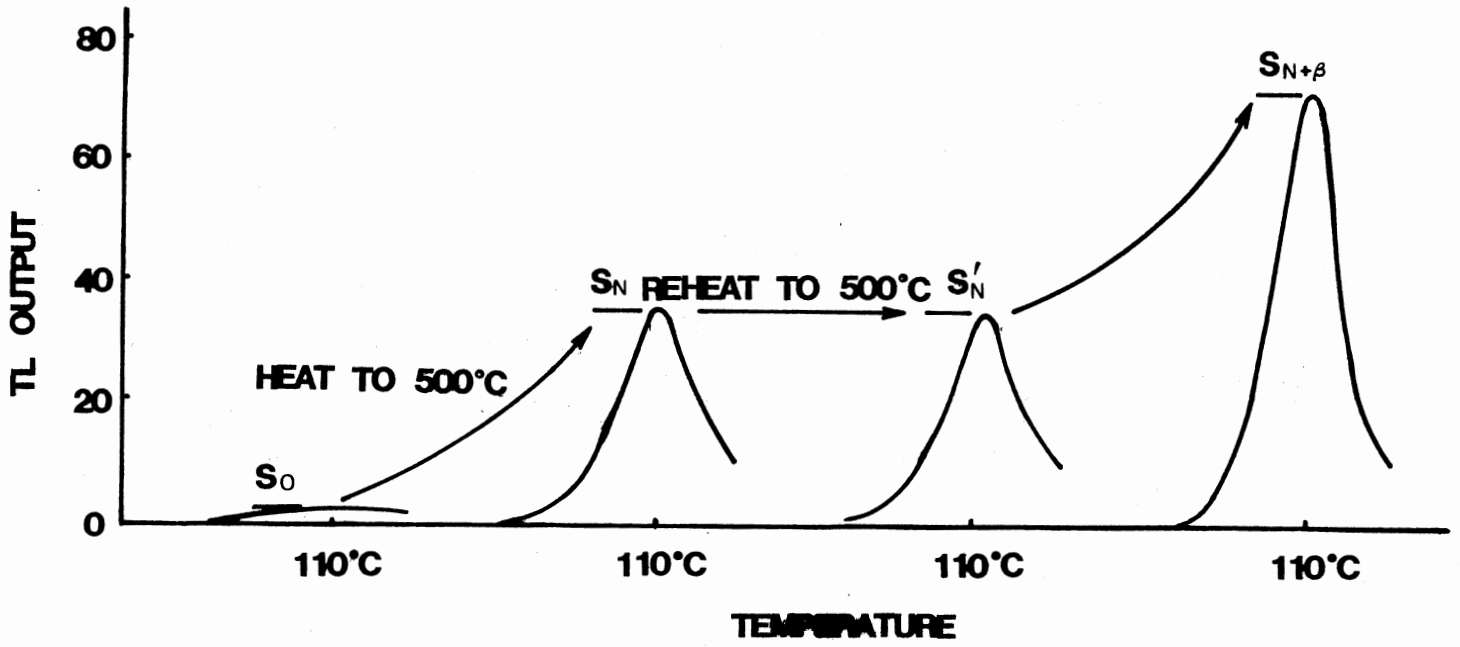

Figure 1. Procedure for the Determination of the TL Sensitivity of the 110°C Peak of Quartz under Various Conditions of Heat Treatments and Pre-Dose

Gy test dose irradiation is also seen to give the same sensitivity, denoted here by S_N'. If the sample is now given a large dose β (say, several Gy) and is again heated to 500 °C to drain the TL associated with the 110 °C peak, then, on subsequent irradiation with the 1×10^{-2} Gy test dose, an increased sensitivity of $S_{N+\beta}$ is obtained.

Three important features can be observed here: 1; $S_o = S_N'$. This implies that heating to 500 °C alone does not cause any increase in sensitivity. 2; the growth from S_N' to $S_{N+\beta}$ is related to the dose β. 3; the growth from S_N to S_o is related to the pre-dose N. Assuming a linear relation, we have

$$\frac{N}{S_N - S_o} = \frac{\beta}{S_{N+\beta} - S_N'}$$

So

$$N = \beta (S_N - S_o)/(S_{N+\beta} - S_N') \qquad (1.1)$$

It is assumed that the sensitivity S_o is the original sensitivity of the sample before the pre-dose N is given. In this way, the pre-dose technique can be used to calculate the original unknown dose N.

The Pre-Dose technique has long been used by the archaeometry community to determine doses absorbed by ancient pottery samples; this, in turn, is used to determine their age (2). Natural quartz is commonly present in the pottery samples and by utilizing the Pre-Dose technique the dose delivered to the sample can be estimated. Since the

artifact was fired in ancient times, the dose delivered to it since firing can be used to estimate the age since firing.

In recent years, one often meets with such dosimetric situations in which the radiation field is no longer present and one wishes to know retrospectively what the delivered dose was during the period of exposure. In such instances, prepared samples of suitable material are not available for TL measurement and, instead, one has to rely on the use of natural materials which were present at the time of the radiation. Examples of such instances include the accidental exposure of personnel or objects to radiation sources and the assessment of the dose delivered to people and to the environment during the use of nuclear weapons. In these cases, the Pre-Dose technique is a popular option because natural quartz is easy to find in building materials and because the Pre-Dose technique is very sensitive. It can provide an estimation of the dose as small as 0.05 Gy.

Zimmerman's Model

The only model existing which attempts to explain the experimental observations of the Pre-Dose Effect was proposed by Zimmerman (3). From combined measurements of radioluminescence (RL), thermally stimulated exo-electron emission (TSEE) and TL, she concluded that not only is the sensitivity enhancement of the TL observed after both irradiation and heating treatment, but also that the effect

can be reversed by UV irradiation (230-250 nm) and it is the luminescence centers, not the traps, that have been affected. The mechanism suggested by Zimmerman is shown in figure 2. There exist in the energy gap electron traps T_1 and T_2, and recombination centers L and R. T_{o1} is the shallow trap which is responsible for the 110 ^{o}C TL peak. Trap T_2 is introduced into the model to maintain the charge balance. It is assumed that T_2 is deep enough as not to be emptied by heating to 500 ^{o}C. For conceptual ease, the positively charged luminescence centers are regarded as containing captured holes. Holes trapped at L act as luminescence sites for the 110 ^{o}C TL emission and holes at R function as non-luminescence sites and are termed as reservoir centers. During the TL process, electrons are thermally released from the traps T_1 and some of them are captured at the luminescence centers. Such a capture only occurs for centers which are charged with a hole and so the TL sensitivity is proportional to the number of centers which are so charged.

Firing of the sample is presumed to empty nearly all the centers. An irradiation by a small test dose puts a few electrons in T_1 and holes in L, heating to 110 ^{o}C releases electrons from T_1 and some of them are captured at L to yield a small TL signal of intensity S_0. So the TL sensitivity after firing is low. Pre-Dose irradiation excites electrons to the conduction band from the valence band and leaves holes in the valence band. Then the

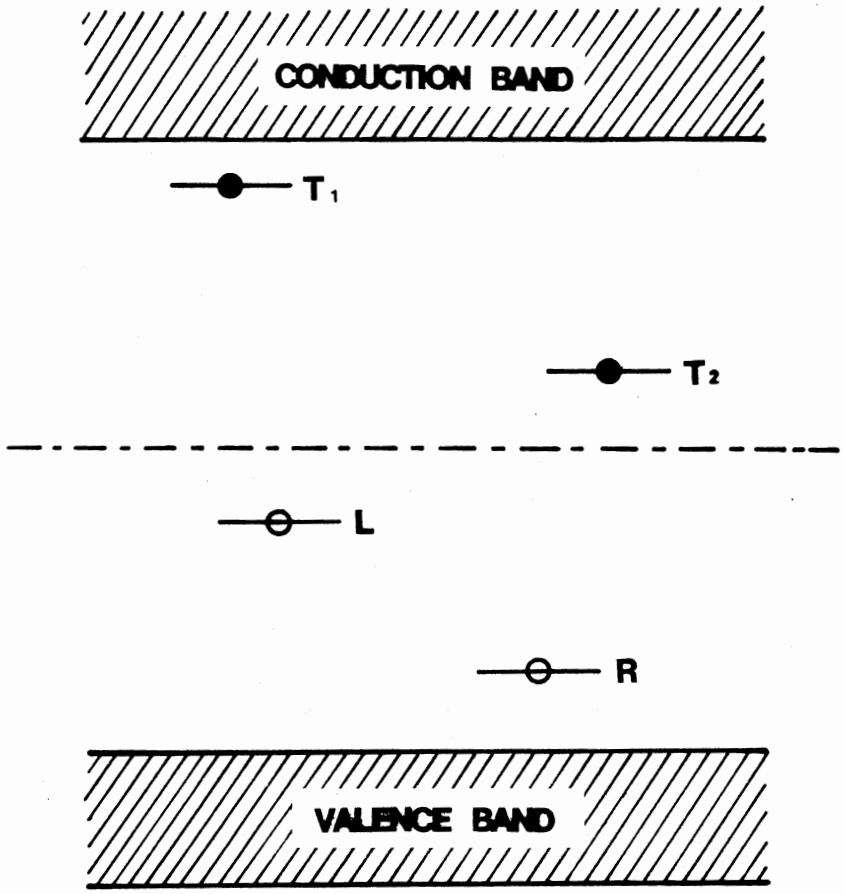

Figure 2. Zimmerman's Model

electrons are trapped in T_1 and T_2. In this model, it is also assumed that the probability of hole trapping at R is much greater than that at L so that holes are captured in R rather than in L. The hole population in R is thus proportional to the Pre-Dose N.

The first step of the Pre-Dose dating procedure is that of measuring S_0. The charge trapped in T_1 is removed by the initial heating to 150 ^{o}C before the Pre-Dose activation. A small test dose charges the trap T_1 with a small number of electrons and puts a small number of holes into L. Electrons are released by heating through 110 ^{o}C and those that find a charged luminescence center give rise to TL. Because that no change has been made to the number of holes trapped at the centers of L, the observed sensitivity S_0 is the same as if the measurement has been made immediately after firing.

In the second step of the procedure, heating to 500 ^{o}C, holes are thermally released from R and some of them are transferred to L. The electrons in the deep centers T_2 remain unaffected. Hence, when the sample is cooled to room temperature a significant number of holes now populates L such that after test irradiation there are more holes in L with which the electrons thermally released from T_1 could recombine. When the sample is now heated through 110 ^{o}C, a large TL peak of intensity S_N is produced. Thus, in this model, the pre-dose N is seen to affect the number of holes in R, whereas heat treatment transfers holes from R to L.

The number transferred depends on the number present in R, which in turn depends on the pre-dose N.

Some Complications of Pre-Dose Dating

Although the technique of Pre-Dose dating has been widely used in TL dosimetry, there are still a lot of complications and uncertainties which occur frequently during the application of the technique and which can not easily be explained on the basis of the simple model discussed above. One of these problems is the uncertainty in the thermal activation of the Pre-Dose Effect. The procedure for the activation suggested by Fleming (4) was a single rapid heating of the sample to 500 ^{o}C. This temperature was chosen because it achieves the maximum sensitivity increase. Chen (5), however, noted that in many cases a higher activation temperature is required to achieve the maximum enhancement. In some instances, it becomes necessary to heat the sample beyond the alpha-beta transition point (573 ^{o}C) before the maximum increase is achieved. Heating beyond the alpha-beta phase transition point can introduce profound changes in the TL glow curve of quartz (6-7). One interpretation of this (8) concerns the formation of metastable defect clusters which lead to a change in the TL properties. The alteration in the defect structure by heating above the phase transition may have a major effect on the activation of the Pre-Dose mechanism. The alteration may involve changes in the total number of R

centers or of L centers, or of the R center activation energy distribution. To be certain about all these problems a detailed knowledge of the defects involved in the Pre-Dose phenomenon is required.

Additional to the above difficulty, unwanted sensitization effects have also received attention. A recently reported observation by McKeever (9) and by others (7) concerns a small increase in sensitivity of the 110 ^{o}C peak following heating alone for some quartz samples. The cause of this is unknown but it appears to be related to an enhancement of the recombination probability at L centers (9).

For some samples it is reported that heating beyond 500 ^{o}C causes a decrease in the 110 ^{o}C peak sensitivity (10). This effect is termed "thermal deactivation" and its cause has not yet been pinpointed (11), although it has been interpreted, in terms of Zimmerman's model, to be due to the thermal excitation of holes from L centers.

When we use equation (1.1) to evaluate the pre-dose N, a linear relation between pre-dose and sensitivity has been assumed. However, it is often found that the sensitization of the 110 ^{o}C peak does not exhibit a linear relation with pre-dose. In particular, sublinearity is often observed, for which there may be several causes. Aitken and Murray (12) note that the value S_N' is often less than S_N (refer to figure 1). Termed "radiation quenching", this appears to indicate a neutralization of the holes in L by electrons.

This would give rise to a non-linear relationship between the pre-dose and the sensitization. Aitken and Murray (12) suggest a correction procedure to account for it, assuming the Zimmerman model for the "Pre-Dose" Effect. However, without a knowledge of the actual mechanism by which the effect is occuring it can not be certain that the correction procedure is effective.

Chen (5) uses a graphical procedure to correct for the non-linear effects by adopting a saturating exponential expression to relate the sensitization to the pre-dose. This procedure too is based closely on the Zimmerman model. Thus, once again it relies heavily on a knowledge of the exact model for the "Pre-Dose" mechanism.

Possible Point Defects Responsible for the Pre-Dose Effect

From the above argument, we see that although Zimmerman suggested a phenomenological model for the Pre-Dose process which is based on a simple energy band model, there have been no discussions of the actual point defects involved in the process. For the practical use of the Pre-Dose dating, there are still some complications which can not be explained by Zimmerman's model. It therefore becomes necessary to conduct a thorough study concerning the point defects which are responsible for the Pre-Dose Effect in order to better understand the process.

The basic structure of alpha quartz consists of SiO_4

tetrahedra which share each of their corners with other such tetrahedra. Due to its unique structure, quartz contains many point defects formed either during growth or by radiation. Basically, they can be classified into three main groups: aluminum-associated, hydrogen-related and oxygen-vacancy type (13).

After a combined study utilizing TL and ESR, McKeever et al (14) suggested that TL is produced at 110 °C when electrons are released from $Ge^{4+} - e^-$ (i.e., $(GeO_4)^-$) centers to recombine with trapped holes at $Al^{3+} - h^+$ (i.e., $(AlO_4)^o$) center and at unidentified hole centers to produce emissions of 470 nm and 380 nm, respectively. They demonstrated that it is the emission at the unknown centers which are predominantly responsible for the Pre-Dose Effect. On the basis of the observed results they suggested that several defect reaction paths were possible over the temperature range of interest. These reactions are shown below where $U\text{-}h^+$ is the unidentified hole trap.

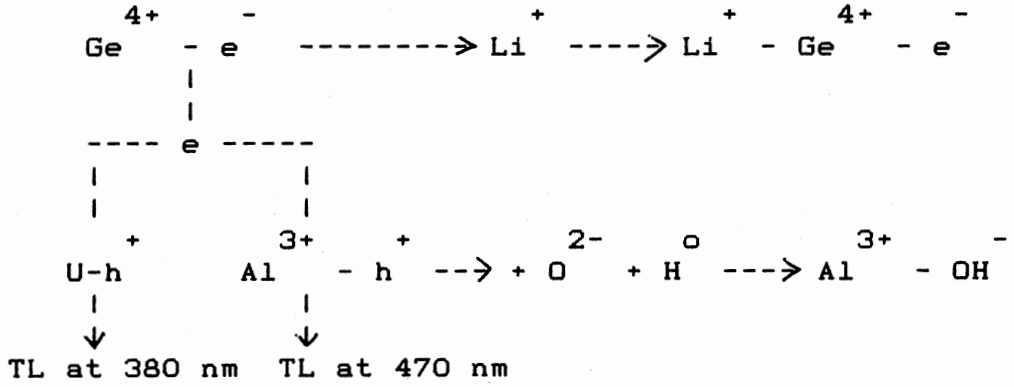

Present Study

In this thesis, we continue an examination of the

Pre-Dose Effect by re-examining the model given above. To achieve this, we have used Thermoluminescence (TL), Electron Spin Resonance (ESR) and Infrared Absorption (IR) techniques to monitor the changes in the concentrations of various defects in quartz samples in response to heating treatments and irradiations. Our main effort is to come up with a point defect model to describe the Pre-Dose Effect, which, in turn, could be used to improve the technique.

CHAPTER II

THERMOLUMINESCENCE

In this chapter, we present TL results for the quartz samples. We have investigated the general TL characteristics of different kinds of quartz samples available after irradiation at room temperature or liquid nitrogen temperature. Also, we have concentrated on two synthetic samples and one natural sample to study the Pre-Dose properties associated with the 110 ^{o}C peak. In this study, we have measured the irradiation dose dependence of the TL intensity, the thermal activation curve (TAC) for the Pre-Dose Effect and the Pre-Dose dependence of the sensitivity. The samples used have been thermally annealed at different temperatures and the effects of annealing are studied. The TL results are explained using point defects.

Experimental Apparatus

A block diagram of the apparatus used to measure the TL signals is shown in figure 3. The TL chamber contains the heater and it is connected to a vacuum pump and a N_2 gas tank. The TL readout is taken in a nitrogen atmosphere and the operational pressure is ~ 600 torr. A Daybreak 520 temperature controller is used to maintain a constant heating rate (usually chosen between 2 - 6 ^{o}C/s). A

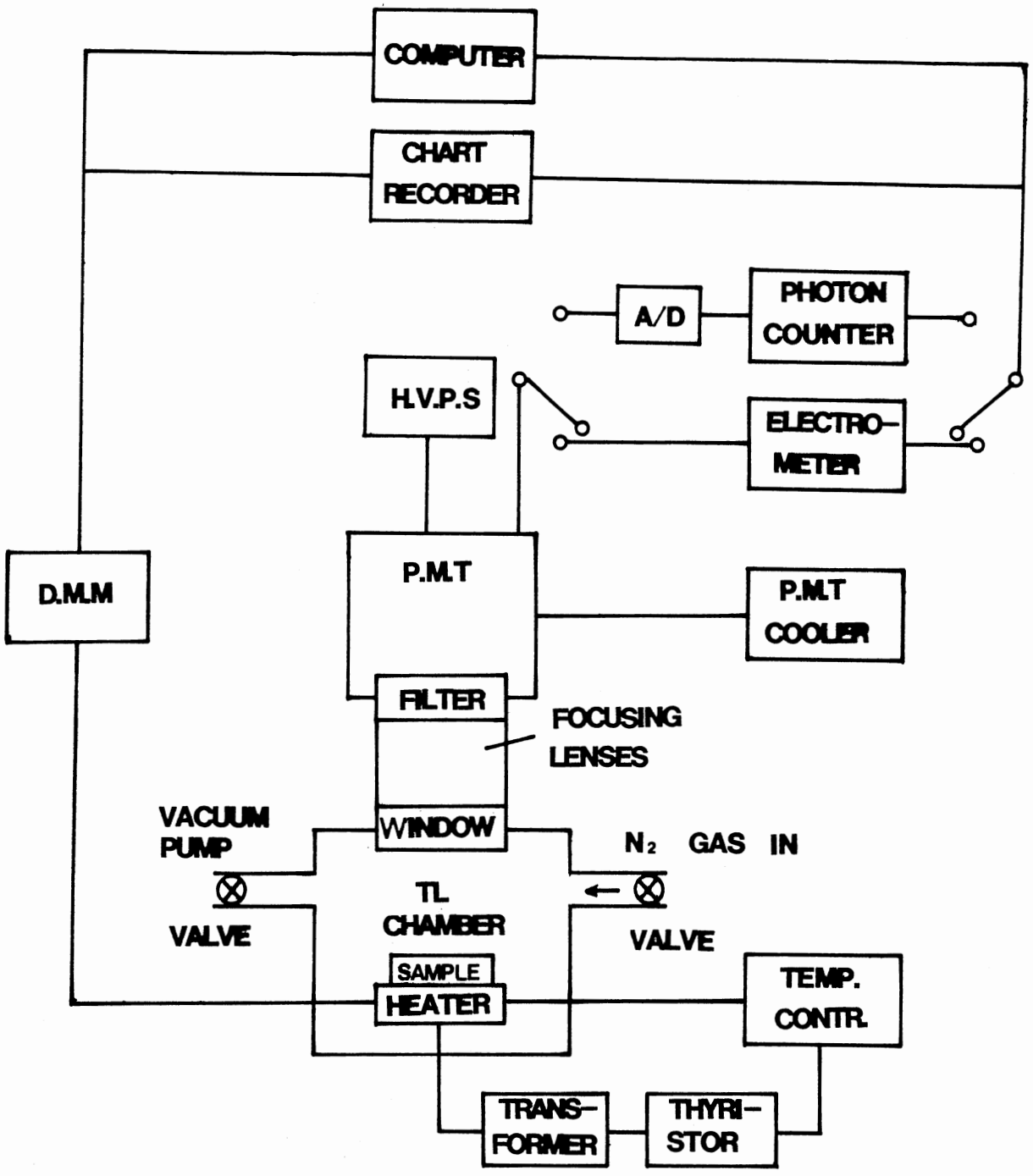

Figure 3. A Block Diagram of the TL Set Up

photomultiplier tube, PMT(9558QB) is used to measure the intensity of the TL. The emitted light is collected through two converging lenses to get an optimum light collection efficiency. A high voltage DC power supply is used for the PMT. A FACT 50 MKIII Thorn EMI Gencom Cooler is used to cool the PMT to -20 ^{o}C to reduce the noise-to-signal ratio. A digital multimeter is used to measure and to display sample temperature using a Chromel-Alumel thermocouple. The PMT can operate in two different modes: D.C. current and photon counting. The TL data is recorded on a chart recorder and can simultineously be stored in the computer (HP86).

Procedure

The quartz samples used in this study were from a variety of sources. Synthetic materials were obtained from Saywer Research Products Inc., Eastlake, Ohio. These were single crystals of Premium Q and Electronic Grade alpha quartz. Y-cut plates were sawn from the bulk samples from both the X- and Z-growth regions.

The natural samples available were from Alaska, Oklahoma, Arkansas and several small pieces of quartz from unknown origins. From a general survey of the TL glow curves, we found that all the natural samples have similar TL properties. As a representative, we choose the Arkansas sample in this study because of the good sample quality available.

Most of the irradiations were carried out using a ^{90}Sr beta source. Different doses were achieved by using both different irradiation times and by placing the sample at different distances from the source. Some measurements were also made following irradiation with a ^{60}Co gamma-source. The results were found to be basically the same, independent of the types of irradiation.

Since quartz is a very hard material, it is difficult to cut it into tiny pieces (about 10 milligrams) in a good, uniform shape required for the TL measurements. We use powder samples, instead. The quartz samples were crushed, ground and sieved, grain sizes of 110 - 250 m (140 -160 mesh) being used in the measurements. Five to fifteen milligrams of powder were placed in a stainless steel dish which, in turn, was placed on a nichrome heating strip. The heating was performed in a nitrogen atmosphere. The filling with N_2 gas ensures a uniform heating environment surrounding the sample and avoids possible oxidation reactions inside the chamber. During heating, the TL intensity versus temperature, known as a "glow curve", is recorded.

For high temperature annealing, the samples were annealed in air in a tube furnace and held at the desired temperature for one hour, and subsequently allowed to cool to room temperature slowly by turning off the furnace power. For "firing" of the sample, the annealing temperature is $950\ ^{0}C$.

Results and Discussion

Basic Glow Curve Description

Some typical TL glow curves of the quartz samples are shown in figure 4. The samples have been fired and given a gamma irradiation of dose about 4.4 Gy at room temperature. Curves (a), (b), and (c) represent Premium Q Z-growth region (PZ), Electronic Grade Z-growth region (EZ) and natural Arkansas quartz, respectively. In each curve a well distinguished peak positioned at ~ 100 ^{O}C is observed. For the synthetic samples, there is also a shoulder around 180 ^{O}C. This may be another peak or several peaks overlapping each other. For the natural quartz, however, the glow-curve seems very "clean" in this temperature region. The shoulder is very small and far away compared with the main peak, and therefore we use the peak height of the main peak as a measure of the TL intensity.

In this figure we demonstrated just the Z-growth samples. For the X-growth region samples, the peak is similar except that it is more intense. (This is due to more impurities present in the X-growth region. This, in turn, implies that the TL is impurity controlled.)

In figure 5, the glow curves of the EZ sample are shown for both irradiation at room temperature and at liquid nitrogen temperature (77 K). From the figure we see clearly that the main peak drops while the second peak keeps almost unchanged upon 77 K irradiation. This happens also to the

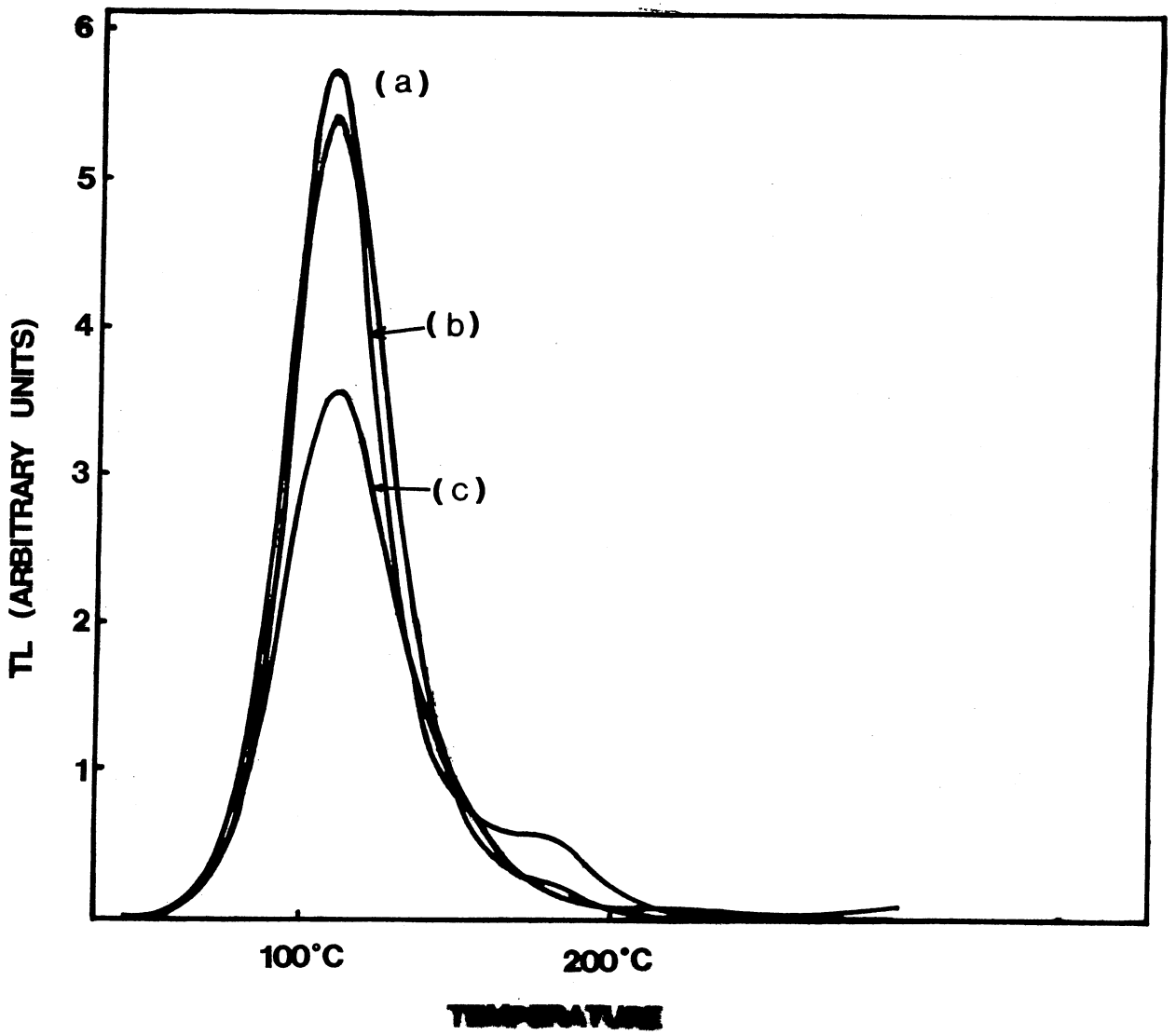

Figure 4. Typical Glow Curves of Fired Quartz Samples Following an Irradiation at Room Temperature, Curves (a),(b), (c) Corresponds to PZ,EZ, and Arkansas Samples, respectively

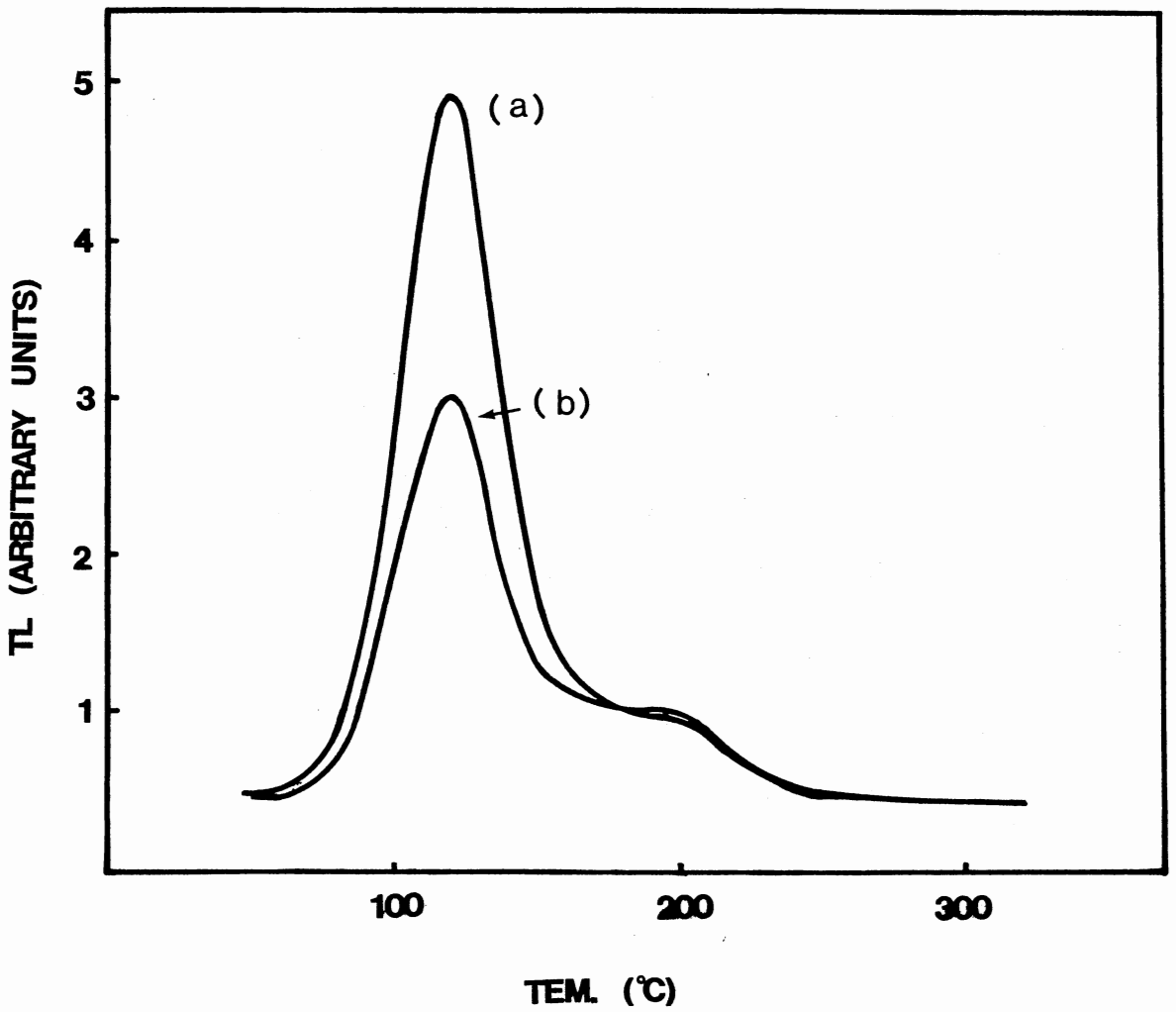

Figure 5. Glow Curves of Fired EZ Samples after a Gamma Irradiation at Room Temperature (a) and at 77K (b)

other samples. Durrani, et al (15) noticed a similar dependence of the TL sensitivity upon the irradiation temperature in the glow curve interval 240 - 420 ^{O}C. The TL emission in this temperature region is believed to be due to the recombination of thermally released electrons at luminescence centers which are considered as (AlO_4^{O}) centers (16-17). Before irradiation, the aluminum is compensated by a monovalent alkali ion. The conversion of this center to the (AlO_4^{O}) center is dependent upon the mobility of the alkali ion. At low temperature irradiation, when the alkali ion is immobile, not many (AlO_4^{O}) centers are produced and therefore the TL intensity is low. We think that this explanation also suits for our observation. This is consistent with the model given by McKeever et al (14) mentioned in chapter I, concerning the role played by (AlO_4^{O}) centers in the TL in this temperature range.

Figure 6 shows the glow curves of the as-received samples after irradiation at room temperature. The synthetic quartz seems to have no high temperature shoulders now. The natural quartz has another glow peak at about 260 ^{o}C of a higher intensity than the 100 ^{o}C peak. Irradiation at 77 K produces similar patterns with a smaller sensitivity.

The effect of pre-irradiation firing deserves emphasis. As an example, we plot in figure 7 the glow curves of a PX sample for both before and after firing. Comparing the two curves, we can see several interesting features. 1), the

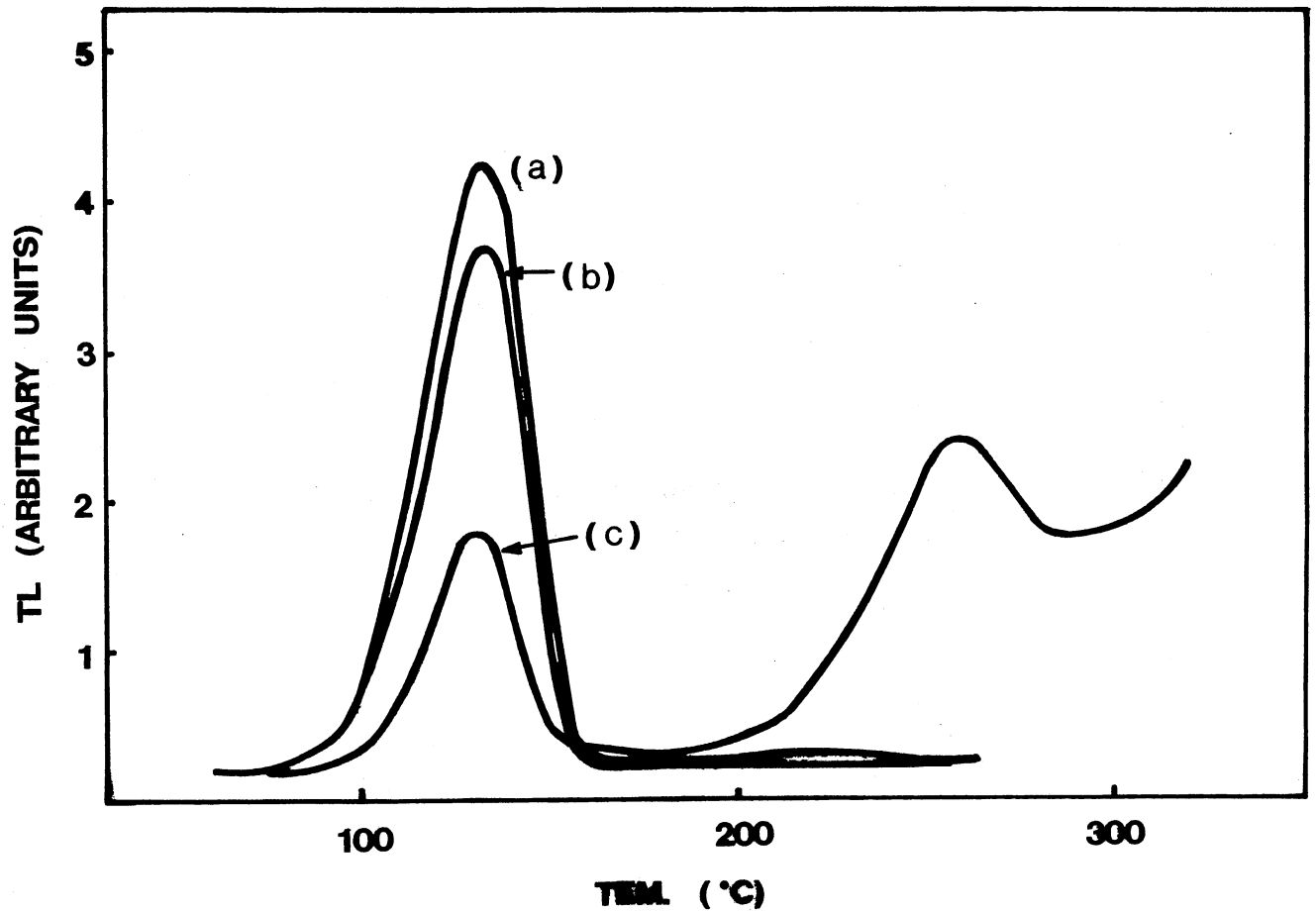

Figure 6. Typical Glow Curves of As-received Quartz Following An Irradiation at Room Temperature, Curves (a), (b) and (c) Are for EX,PX and Natural Arkansas Samples,Respectively

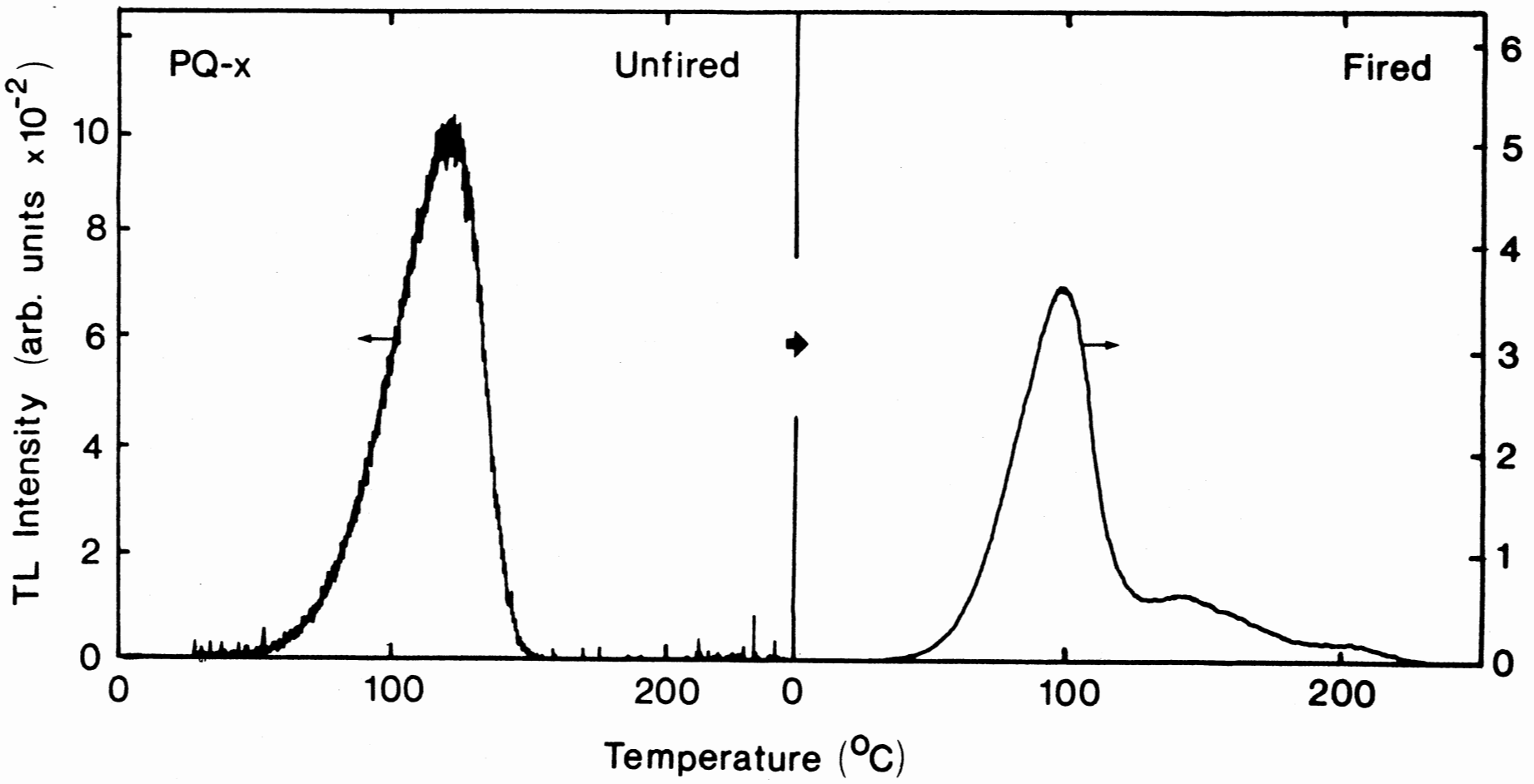

Figure 7. TL Glow Curves from Fired and Unfired PX Samples

sensitivity of the fired sample is greatly increased (here about 40 times). 2), the peak position of the fired sample shifts to lower temperature. For the PX sample, the peak shifted from about 130 to 105 ^{o}C after firing. As mentioned in the above paragraphs, we also note that some higher temperature peaks (~ 180 ^{o}C) are becoming visible relative to the 100 ^{o}C main peak. Similar observations were made for the other quartz samples.

The effect of the firing process on the TL sensitivity can be illustrated by examining figure 8. Here we plot the increase in the sensitivity of the TL peak (expressed as a ratio of the TL from a standard test dose after annealing at 950 ^{o}C to that before the anneal) versus the original TL sensitivity. First, it can be seen that in some samples an increase by a factor of 10^{3} is observed. Even the smallest increase observed is still by a factor of about 30. Secondly, we note that there appears to be an inverse correlation between the increase due to the firing and the original sensitivity.

A similar "anti-correlation" between TL sensitivity and the Pre-Dose Effect was observed by Martini et al (18) for different samples or for a single type of quartz with different treatments. That is, if a sample has a high initial TL sensitivity, it will have a low Pre-Dose Effect and vice versa. This suggests that the firing and Pre-Dose treatments may be having similar effects on the quartz samples.

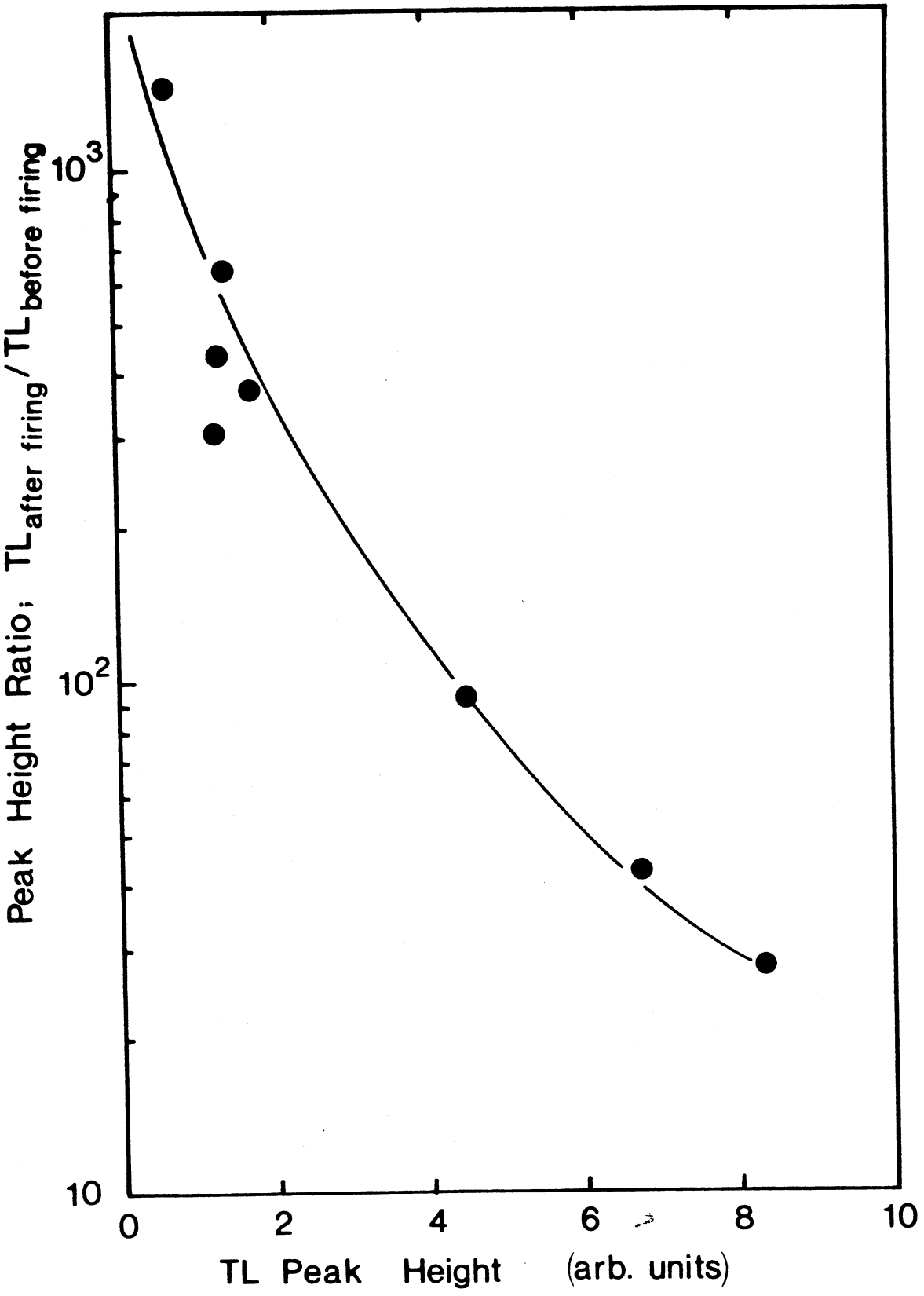

Figure 8. TL Peak Height Ratio versus the Original TL Peak Height for Both Synthetic and Natural Samples

This very strong sensitization by firing was actually reported by David (7) in geological quartz, although in his case the effect was smaller. The smallness of the effect is perhaps due to the fact that the geological samples may have already been partially fired in nature.

An air-swept PQ sample was also examined. The effect of the sweeping is shown in figure 9. Qualitatively we see similar features to the fired sample, namely that the TL peak has shifted to lower temperature, the sensitivity of the peak has been increased, and new peaks appear at higher temperature regions. Air-sweeping moves interstitial alkali ions out of the sample and moves hydrogen ions into it. The sweeping of the sample was performed by Sawyer and the precise conditions of the sweeping are unknown to us. However, usually the sweeping takes place at temperatures of $400^{o}C$ or above. We have already discussed how the sensitivity can be affected by annealing and so it is difficult to separate the effects of ion-exchange and heating in the sweeping process.

Martini et al (18) have provided evidence that the Pre-Dose Effect is present only in unswept or partially swept quartz. They have also given evidence that hydrogen sweeping and the Pre-Dose treatment produce similar effects on the glow curve (19). Since one effect of sweeping is the substituting of alkali ions by hydrogen ions at the Al site, it is possible that the Pre-Dose treatments also have the similar effects of moving hydrogen ions around in the

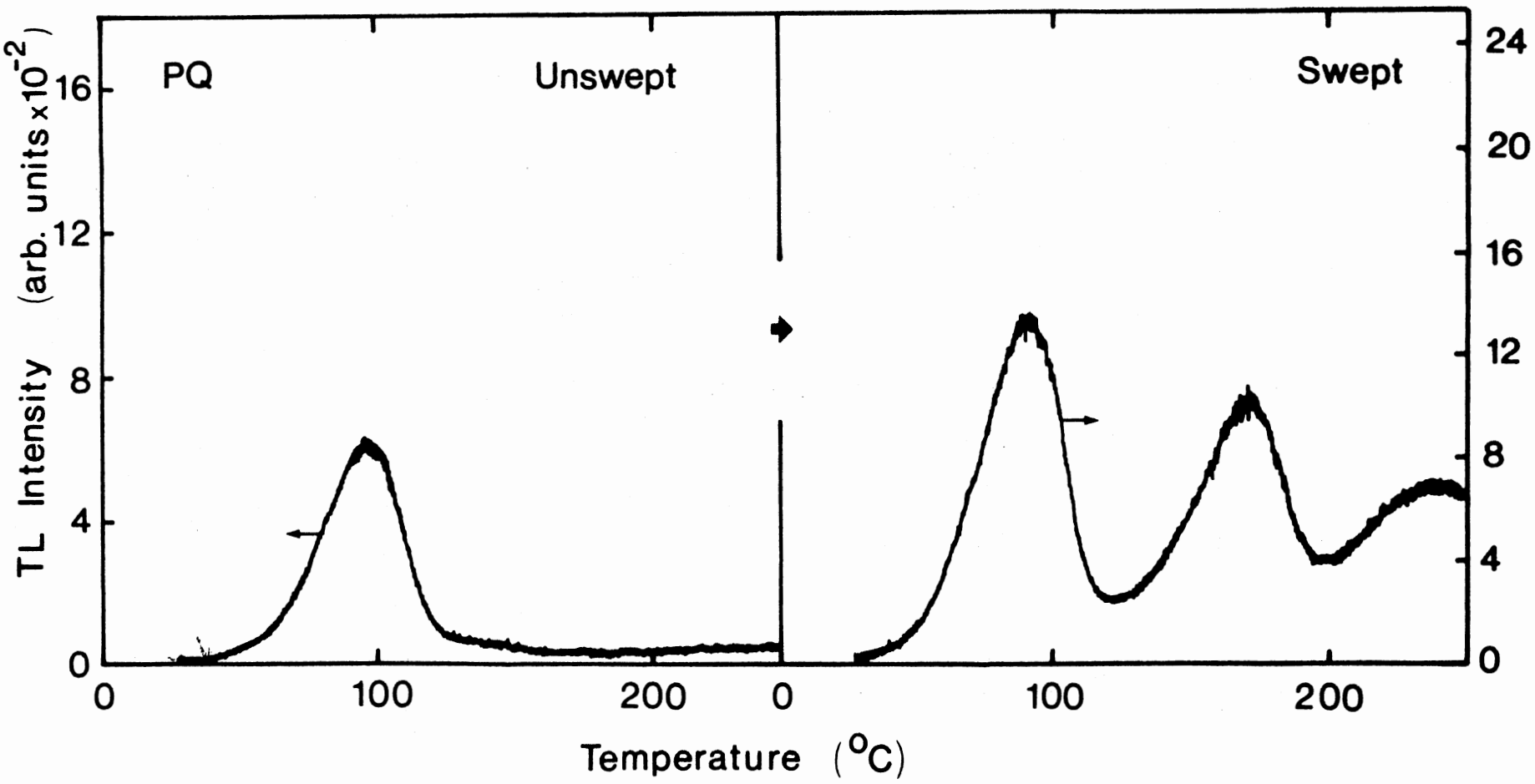

Figure 9. TL Glow Curves from Unswept and Air-Swept Samples of Premium Q Quartz

sample. Since a swept sample will have already saturated these effects, further Pre-Dose treatments would cause no more effects. The suggestion that the TL in the room temperature to 200 ^{o}C region is related to hydrogen was also given by Jani et al (20) from the results of sweeping experiments. We further suggest, from above discussion, that hydrogen ions not only play an important role in producing 100 ^{o}C main peak, but are also a vital component of the Pre-Dose Effect.

Growth Curves

As representatives, we plot the TL intensity versus dose for PX and PZ samples in figures 10 and 11, respectively. We use a log-log scale so that a linear growth is given by a straight line with a slope of one. A superlinear or sublinear relation is represented by a straight line with a slope of γ , with γ greater or smaller than one. The TL data are normalized to the weight of the samples.

The very strong superlinearity with a slope of almost 3 can be seen easily in curve A of figure 10. This is for the as-received PX sample. Curve B gives the result for the fired specimen, showing a linear dose dependence. The fired sample has a much more intense signal compared with unfired one, especially in the low dose region. Also to be noted is the shifting of peak temperature: for unfired samples it varies between 130 ^{o}C and 150 ^{o}C, depending on dose (averaging

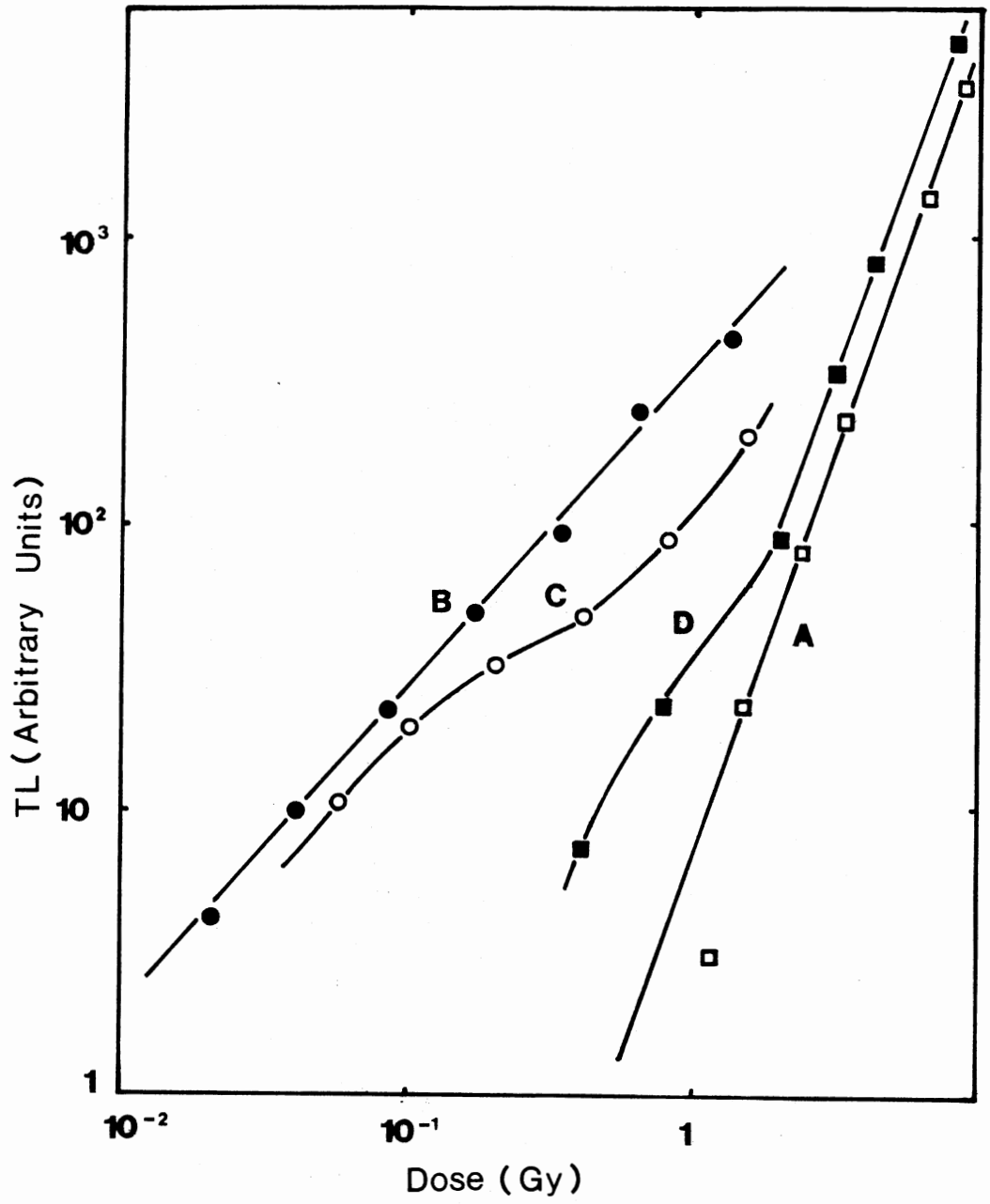

Figure 10. Growth Curves for Various Samples of PX Quartz

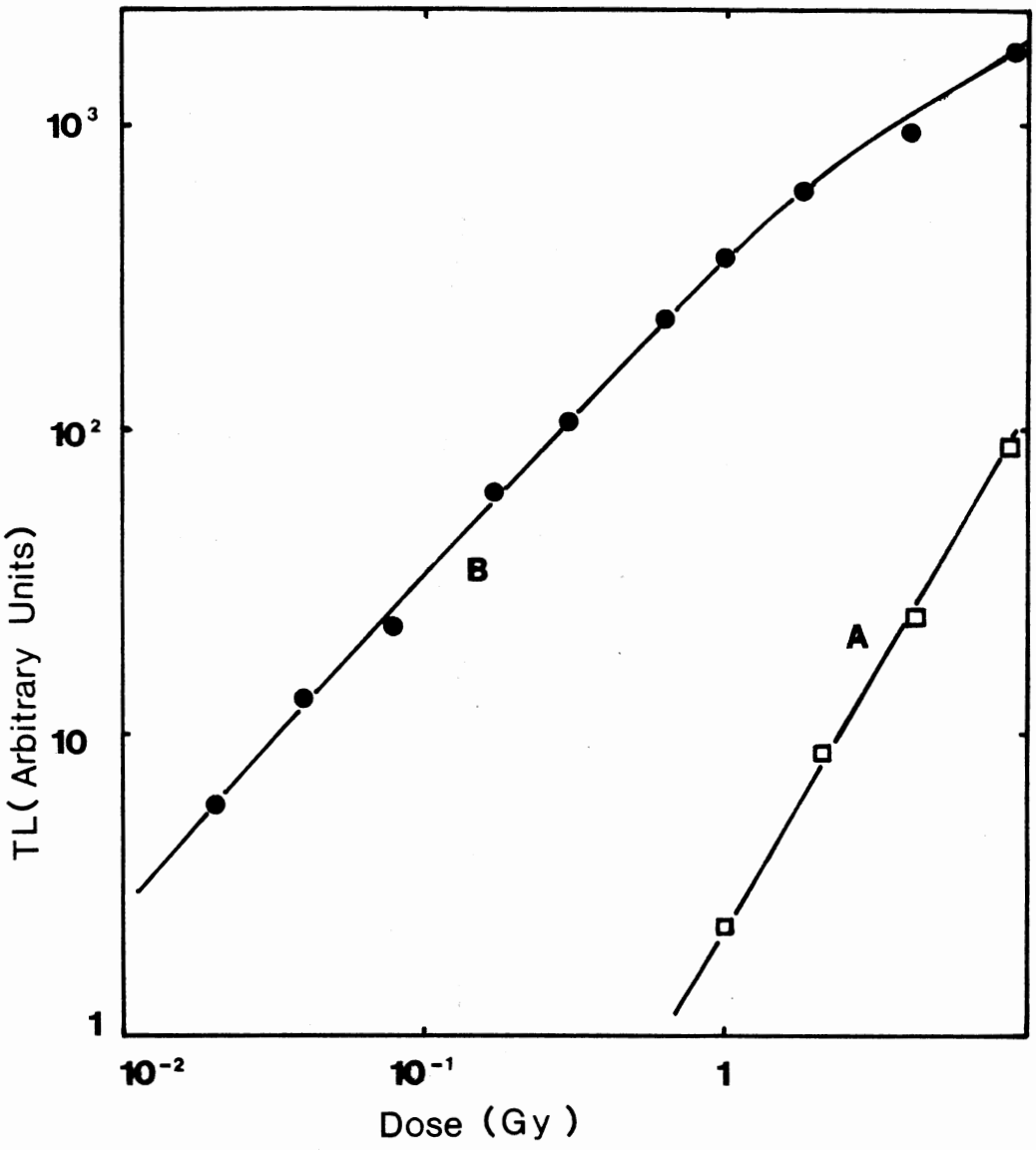

Figure 11. Growth Curves for Samples of PZ Quartz

at 140 °C) whereas for fired samples it changes between 110 °C and 118 °C.

The dose dependence measurements were repeated for the samples annealing at different temperatures. Curve C in figure 10 is for a sample fired only to 300 °C. It starts with a linear relation and then comes a sublinear-to superlinear transition at higher doses. This peak appears at about 120 °C. Curve D in figure 10 shows the dose dependence of the sample fired to 250 °C. Strong superlinearity is still seen at high doses. At lower doses, the trend towards a linear relationship can be seen. The temperature of the peak in this case averages at 128 °C. These results reveal that the transition from strong superlinear to nearly linear behavior occurs around 300 °C.

The same measurements have been done for the other samples. Generally speaking, the results give a superlinearity for the unfired synthetic specimens with a slope close to 2 and a nearly-linear relation for the fired synthetic samples and natural Arkansas sample. Figure 11 shows the results for the PZ sample. Curve A of figure 11 is a straight line with a slope of about 1.7. This is for the unfired sample. For the fired sample (curve B of figure 11) the linear dose dependence is seen at low doses followed by sublinearity at high doses. The peak temperature for these samples was 131 °C for the unfired specimen and 120 °C for the fired sample.

It is to be noted that a slight superlinearity in the

110 °C peak in fired quartz has already been noticed by Zimmerman (7). Also, a stronger superlinearity has been reported by Ichikawa (21) for a peak near 200 °C in natural quartz. We believe, however, this is the first time the superlinearity for 110 °C peak in synthetic quartz is observed. Aitken (22) noticed that irradiation alone can sensitise some natural quartz sample. That is what happens in synthetic samples also. Superlinearity means, for example, that if two units of dose are given successively, then the sensitivity for the second unit is greater than that for the first one. The sensitivity increase is caused by the first irradiation. This effect is small in geological and archaeological quartz, probably due to a previous firing of the sample.

A competition-during-heating model was first postulated by Rodine and Land (23) to explain quadratic TL superlinearity in ThO_2 samples. This model assumes an extra competitor competing for the released electrons during the heating stage of the TL process. Kristianpollor et al (24) further developed this model to show that quadratic and even stronger superlinearity can be achieved by using this model. They also demonstrated that there exists an unusual dose dependence of the peak temperature, over a certain range of doses. The model fits into the observations here very well and is here used to account for the superlinearity, the sensitization and the temperature shift of the 110 °C peak.

An energy diagram for this model is shown in figure 12.

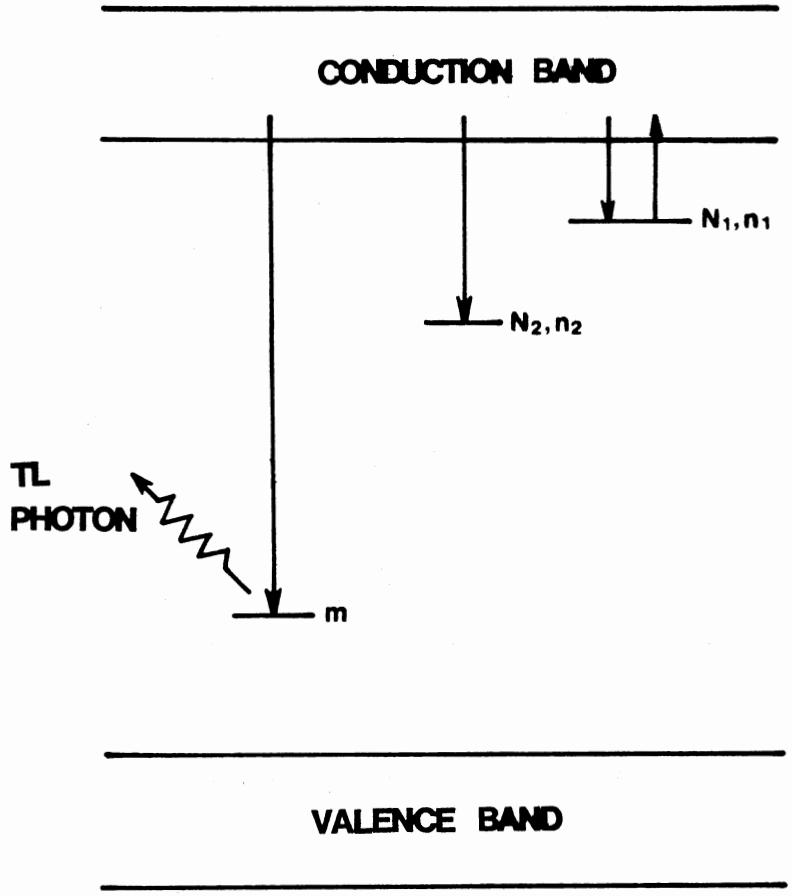

Figure 12. An Energy Level Diagram for Competition-During-Heating Model

In the band gap, there exist N_1 trapping centers and N_2 competing traps per unit volume, of which n_1, n_2 are occupied, respectively. m represents the recombination centers which have trapped holes in them.

During the heating, the concentrations n_1, n_2 and m, as well as n_c, the instantaneous concentration of electrons in the conduction band, are changing with time. It is assumed that the trap centers N_1 is shallow enough so that electrons will be released to conduction band during heating. However, the detrapping of electrons from the competitor is forbidden. The electrons in the conduction band have three reaction paths open to them: recombining at center m, retrapping at the unstable N_1 center or trapping at the competitor N_2. The four simultaneous differential equations governing this process are then

$$\frac{dn_1(t)}{dt} = -r(t)n_1(t) + A_1 n_c (N_1 - n_1(t)) \qquad (2.1)$$

$$\frac{dn_2(t)}{dt} = A_2 n_c (N_2 - n_2(t)) \qquad (2.2)$$

$$I = -\frac{dm(t)}{dt} = A_m m(t) n_c \qquad (2.3)$$

$$\frac{dm(t)}{dt} = \frac{dn_1(t)}{dt} + \frac{dn_2(t)}{dt} + \frac{dn_c(t)}{dt} \qquad (2.4)$$

Here, $r(t) = s\exp(-\frac{E}{KT})$, where E is the activation energy for the release of electrons from the trap, s is the frequency factor and T(t) is the temperature. A_1, A_2 and A_m are the probabilities of retrapping into N_1, trapping at N_2 and recombination at m, respectively. I(t) is the instantaneous TL intensity.

By the usual assumption that $\frac{dn_c(t)}{dt} << \frac{dm(t)}{dt}$,

Kristianpollor et al (24) reached a single differential equation for m(t), namely

$$I(t) = -\frac{dm(t)}{dt} = r(t)Amm(t)F(t) \qquad (2.5)$$

where

$$F(t) = \frac{[(n_{10}+n_{20}-m_0-N_2)+m(t)+(N_2-n_{20})(m(t)/m_0)^{A_2/A_m}]}{A_1(N_1+N_2-n_{10}+m_0)+(A_2-A_1)[m(t)+(N_2-n_{20})(m(t)/m_0)^{A_1/A_m}]}$$

Given a set of initial parameters (n_{10}, n_{20}, m_0) equation (2.5) can be solved numerically and the maximum intensity, as well as the peak temperature, can be evaluated. If a certain dependence of n_{10}, n_{20} and m_0 on absorbed dose is assumed, the calculations can be repeated and the variations of the maximum TL intensity I_m and the temperature of the maximum T_m can be monitored, as functions of dose.

In this way, Kristianpoller et al (24) showed that

strong superlinearity occurs when retrapping into N_2 is relatively strong. If linear dose dependences for n_{10}, n_{20} and m_0 are assumed, the results give a quadratic superlinearity, i.e., $I_m \propto D^2$, and the peak temperature decreases with the dose. However, if a saturating exponential growth such that $n_{20}(D) = N_2[1-\exp(-\alpha D)]$ is assumed (α = a constant) the result is rather different. At low doses the maximum TL intensity increases as a function of D^2, while at higher doses stronger superlinearity is seen. When saturation is reached ($n_{20} = N_2$), the relation becomes linear. Also, the peak temperature increases with the dose initially until the transition point from strong superlinearity to linearity is reached, whereafter it starts to move back to lower temperatures.

Besides the numerical calculations for equation (2.5), an analytical solution is also approached by the latter authors (24) using the same assumption that the competitor retrapping is relatively strong, namely:

$$A_2(N_2 - n_2(t)) >> A_1(N_1 - n_1(t)) + A_m(t) \qquad (2.6)$$

and a weak retrapping, namely:

$$r(t)n_1(t) >> A_1(N_1 - n_1(t)) \qquad (2.7)$$

and a small initial filling of the trap, i.e., $n_{10} << N_1$ and N_2. The result is

$$S = \frac{A_m}{A_2 (N_2 - n_{20})} m_0 n_{10} \qquad (2.8)$$

where S is the area under the TL glow curve.

From this equation we can gain more insights into what is happening since we see that if both m_0 and n_{10} are linearly dependent on dose, and $n_{20} << N_2$, then the TL depends quadratically on the dose. However, if n_{20} is not negligible compared to N_2, then the factor $(N_2 - n_{20})$ is a decreasing function and the dose dependence will show stronger superlinearity.

From above, we see that the competition-during-heating model can explain the superlinearity of the 110 ^{o}C peak. Although the recombination site, as suggested by McKeever et al (14), may be two different defects, namely a $(AlO_4)^{o}$ center and, as yet, an unidentified hole site (referring to chapter I), this model is still applicable.

The existence of the competing trapping center is very important to understand the Pre-Dose Effect. We have introduced Zimmerman's model in chapter I. However, a flaw was pointed by Chen (5). This author pointed out that in Zimmerman's model, the sensitization is caused by recombination centers (via the Pre-Dose treatment) on the one hand, but on the other hand, the increasing of the TL signal with increased test dose means the sensitization is also caused by trapping centers. The dependence of TL sensitivity on both the concentration of electrons and holes

conflicts with the simple fact that normally the TL intensity is proportional only to the smaller of the two concentrations.

The conflict can be removed by introducing an extra competing center N_2. In this case it competes with the holes in M for electrons released from trap N_1 and the TL intensity is dependent on both the number of trapped electrons and the number of trapped holes (see equation (2.8)).

Another possible way to describe the superlinearity behavior is to allow for competition during irradiation (25). If this is the case, we should see the superlinear growth of the defects with irradiation dose which are thought to be responsible for the 100 ^{o}C peak. However, studies of the growth of different defects as a function of dose using ESR have given us simple saturating exponential curves (26). As a result we prefer a model involving competition during heating.

The transition from superlinear behavior to linear behavior after high-temperature firing can be easily explained using the competition-during-heating model. Without the competitor, an ordinary linear dose dependence should be seen. If the effect of annealing to high temperatures is to remove the competitors, then the number of competitors is becoming smaller and smaller and the competition is no longer an important factor. The dose dependence tends to linear. It appears, however, that the

perfect linear behavior is still not reached after the firing to 950 °C and the Pre-Dose Effect is still observed.

Furthermore, the shift of the TL peak to lower temperature after firing can also be explained using the model (24). Intuitively, the partial removal of the competitor makes it easier for the released electrons to recombine at the luminescence center, with the result that the luminescence is seen sooner (i.e., at lower temperatures).

One can also explain qualitatively the increase in sensitivity after firing to high temperatures. When the competitor has been removed by firing, the electrons that would otherwise go to the competing center now go to the luminescence sites, resulting in a increased TL sensitivity.

In the next chapter, we will show the ESR results. We examined the ESR signals from both fired and unfired samples. We were looking for a defect center that increased its concentration after firing so that we could correlate it with the increase in TL sensitivity. However, we failed to find an appreciable increase after firing in any of the defects which are believed to be related to the TL process. These results are consistent with the present suggestion that the TL increase is due to the removal of competitors rather than an increase in the concentration of the defects.

In our ESR study we observed a decrease (by a factor of about 4) in the concentration of E_1' centers following firing. According to the presently accepted model, the E_1'

center is an oxygen vacancy having an unpaired electron. More importantly, it has been found (27) that if the samples are pre-annealed between 300 °C and 400 °C the E_1' centers are not formed. Since this is also the temperature range over which the transition from superlinearity to linearity happens (see figure 10) then one might speculate that these centers fill the role of the competitors in the present model.

One thing that looks puzzling, however, is that the TL sensitivity increases a lot (typically 100 times or more) following firing whereas the E_1'-center decrease is relatively small. There might be two reasons to account for this incompatibility. One is that TL is a much more sensitive technique compared with ESR. A small change detected by ESR may be significant by TL. Another one is that the removal of some competitors could drastically increase the recombination probability which is not just a simple linear relation.

We have mentioned in a previous section that the sweeping and the Pre-Dose treatments have similar effects. Jani et al (27) also noted that the E_1' centers can be found only in unswept or partially swept quartz. This means that the E_1' centers can be easily formed only when interstitial alkali ions are present in the crystal although a detailed knowledge of the process is not known. When the hydrogen ions are present instead of alkali ions, the formation of competitors is difficult, as a result, the TL signal is big

and the Pre-Dose Effect is small.

Finally, we would like to point out that the recognition of E_1' as the competitor is just a speculation. The production process used by Jani et al (27) reveals that room-temperature irradiation by itself does not readily form E_1' centers, whereas a thermal anneal at 300 °C following an irradiation at room temperature enhances the E_1' center concentration at least by a factor of 20. These results suggest that the formation of the E_1' center is a two-step process. The initial room temperature irradiation changes "precursor" defects present in an as-growth crystal into an intermediate state which is then converted into E_1' centers by the subsequent anneal at 300 °C. The 300 °C anneal in the production of E_1' center renders the E_1' as competitors questionable since the E_1' precursor center may not be present in as-growth samples. So the task of looking for the competitor is still before us. The competitor should have the similar features to the E_1' center except that it must be present in as-grown samples.

Pre-Dose Characteristics

As an experimental routine, we have tested the Pre-Dose Effect on fired synthetic samples following Fleming's procedure (4). We did not do this test for unfired samples because irradiation alone will increase the sensitivity (i.e., superlinearity), so it is difficult to distinguish between this and the Pre-Dose Effect.

The procedure uses a test dose of 6.8×10^{-3} Gy beta irradiation and the Pre-Dose used is about 1 Gy. In general, we found that for both PX and EX samples, the Pre-Dose Effect is very small (sensitivity increased by a factor of about 3) compared with the geological samples. This means that after firing at 950 ^{o}C, there still exists enough competitors to give rise to the Pre-Dose Effect. This is consistent with the conclusion from the previous section. Geological quartz, however, may have been partially fired or, if fully fired, may have partially relaxed towards its original state over its geological life time. Another possibility which we will discuss later is that since the Pre-Dose Effect is relatively small for a newly fired sample, some hydrogen ions may have diffused into the sample so that the Pre-Dose Effect is nearing saturation. Further experiments are needed to verify this speculation.

In order to see over what temperature range the Pre-Dose Effect is activated, the sample's "thermal activation curve" (TAC) was also obtained. The procedure is as follows. 1). Give a Pre-Dose of gamma irradiation of 11 Gy. 2). Heat the sample to the desired temperature T and quickly cools back to room temperature. 3). Give a test dose of 2.5×10^{-2} Gy and heat the sample just above the peak temperature and record the TL intensity S. 4). Plot S as a function of T.

Curve A in figure 13 is the TAC for a fired PX sample. We can see that the sensitivity starts to increase near

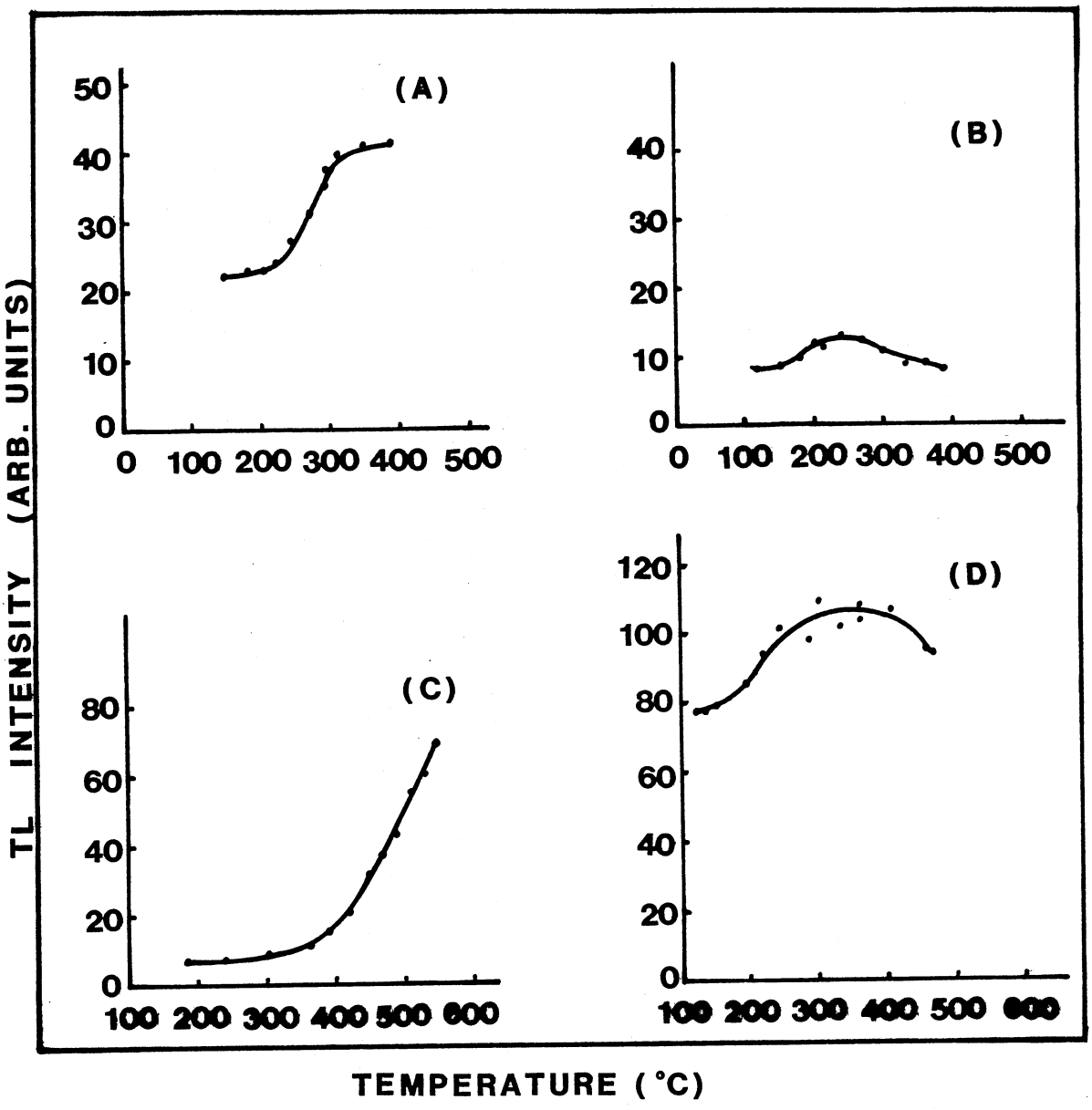

Figure 13. Thermal Activation Curves for Different Samples, Curves (A) and (B) are for Fired PX and EX, Curves (C) and (D) are for Both Unfired and Fired Arkansas Samples

200 °C, reaches a maximum at 300 °C, then stabilizes. Curve B in figure 13 is the TAC for fired EX. In this case, however, the intensity starts going up around 180 °C, reaching a maximum at about 250 °C and then drops to its original level. Curves C and D in the same figure is for unfired and fired Arkansas sample, respectively. It is readily seen that for unfired samples the activation starts at about 400 °C and continuously goes up. For the fired sample, however, the increase starts at about 200 °C and reaches the maximum at about 250 °C.

Two observations should be made for the TAC of the natural sample. (i) The sensitization for the unfired sample is much bigger than that for the fired sample. (ii) The activation happens much earlier for the fired sample. The first observation can be explained by the removal of competitors following firing. For the fired sample, the competitors have been partially removed so that the initial sensitivity is high. For an as-received sample, however, more competitors are present in it and the competitors are being removed during the thermal activation process, resulting in a higher sensitivity increase. So the thermal activation is stronger for the as-received samples. For the second observation, a satisfactory explanation is lacking.

The diversity of the TAC curves for different samples implies that the Pre-Dose process is impurity controlled and is therefore not of purely intrinsic origin as advocated by Martini et al (28). This is consistent with our earlier

suggestion.

The study of the Pre-Dose dependence of the TL sensitivity has also been done for a variety of the samples. The activation temperature is chosen so that the maximum is reached in the TAC. As a representative, figure 14 shows the results for PX and natural Arkansas. Both samples were fired. We can see that the sensitivity increases in the dose range of about 0 to 11 Gy for PX sample and about up to 6.6 Gy for the Arkansas sample. After these values the sensitization saturated.

Summary

From the experimental observations, we found that the effect of the firing, the Pre-Dose treatments and the sweeping of the sample are similar, all appearing to increase the TL sensitivity. The fired or swept samples also seem to have a low Pre-Dose Effect. This "anti-correlation" between the initial TL sensitivity and the Pre-Dose Effect can be explained by two different mechanisms. The effect of firing is to remove the competitors so that the initial sensitivity is high and, as a result, the Pre-Dose Effect is low. Air-sweeping substitutes H ions for interstitial alkali ions. We will see later that ion exchange due to sweeping affects the recombination center ($(H_3O_4)^{o}$). In this way the concentration of recombination centers becomes saturated and, as a result, the Pre-Dose Effect for a swept sample is very low.

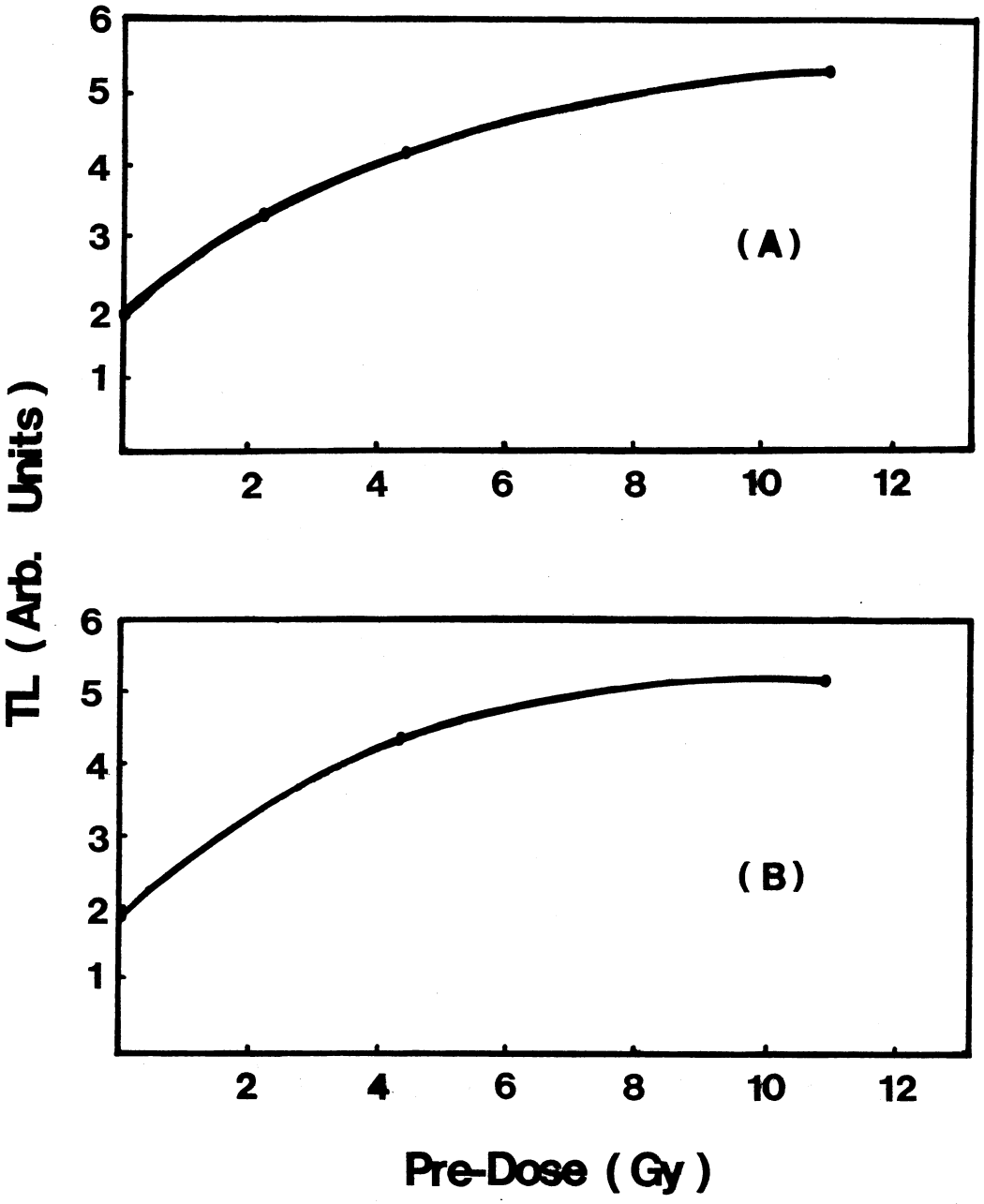

Figure 14. The Plot of TL Sensitivity Following Activation vs Pre-Dose for Fired PX (A) and Arkansas (B) Samples

The superlinear behavior of the growth curves of as-received synthetic quartz is explained via a "competition-during-heating" model. The transition to linear behavior following high temperature annealing suggests that the firing removes competitors from the sample.

CHAPTER III

ELECTRON SPIN RESONANCE

Electron Spin Resonance (ESR) was used as a tool to monitor the various defects which are considered to be related to the Pre-Dose Effect. The samples were subjected to various thermal treatments and correlations between the 110 °C TL peak and the concentration changes of some defects were made.

Experimental Detail

ESR Spectrometer

The ESR results were obtained by using an IBM Instruments (Bruker) ER200D X-band homodyne spectrometer with the sample either at liquid helium, liquid nitrogen or room temperature. The microwave radiation is generated and detected by the microwave bridge. A TE102 rectangular cavity, which was used in this study, was placed in the open space between the two magnets and was connected to a Bruker ER044 MRDH microwave bridge through a waveguide. The TE102 is a commercial cavity with Helmholtz coils for 100 KHz modulation. Besides the magnets, the magnet power supply, and the microwave bridge, the ER200D also contains a main console which consists of a timebase unit, a signal channel,

a magnetic field controller and a chart recorder. A block diagram of the ESR spectrometer is given in figure 15.

Experimental Procedures

For the ESR study, the quartz samples were cut into dimensions of 7 mm x 3 mm x 2.5 mm in the X, Y and Z directions, respectively, by using a diamond saw. Both the X- and Z-growth regions were taken from synthetic samples.

In addition to the ^{60}Co gamma cell, the samples were also irradiated with 1.7 MeV electrons at 10 microamperes from a Van de Graaff accelerator. For irradiation at 77 K, the sample was put inside a styrofoam cup filled with liquid nitrogen.

The variable-temperature-pulse-anneals were done outside the ESR spectrometer by using a tube furnace. Usually the sample was held at the desired temperature for 5 minutes and was taken out of the furnace after it had cooled to room temperature.

The liquid helium temperature measurements were achieved using the liquid transfer Heli-Tran system which provides refrigeration in the temperature range between 4.2 K and 300 K via a controlled transfer of liquid helium. An air products model 3700 digital temperature indicator/controller was used to regulate the temperature.

Results and Discussion

The $(AlO_4)^o$ Center

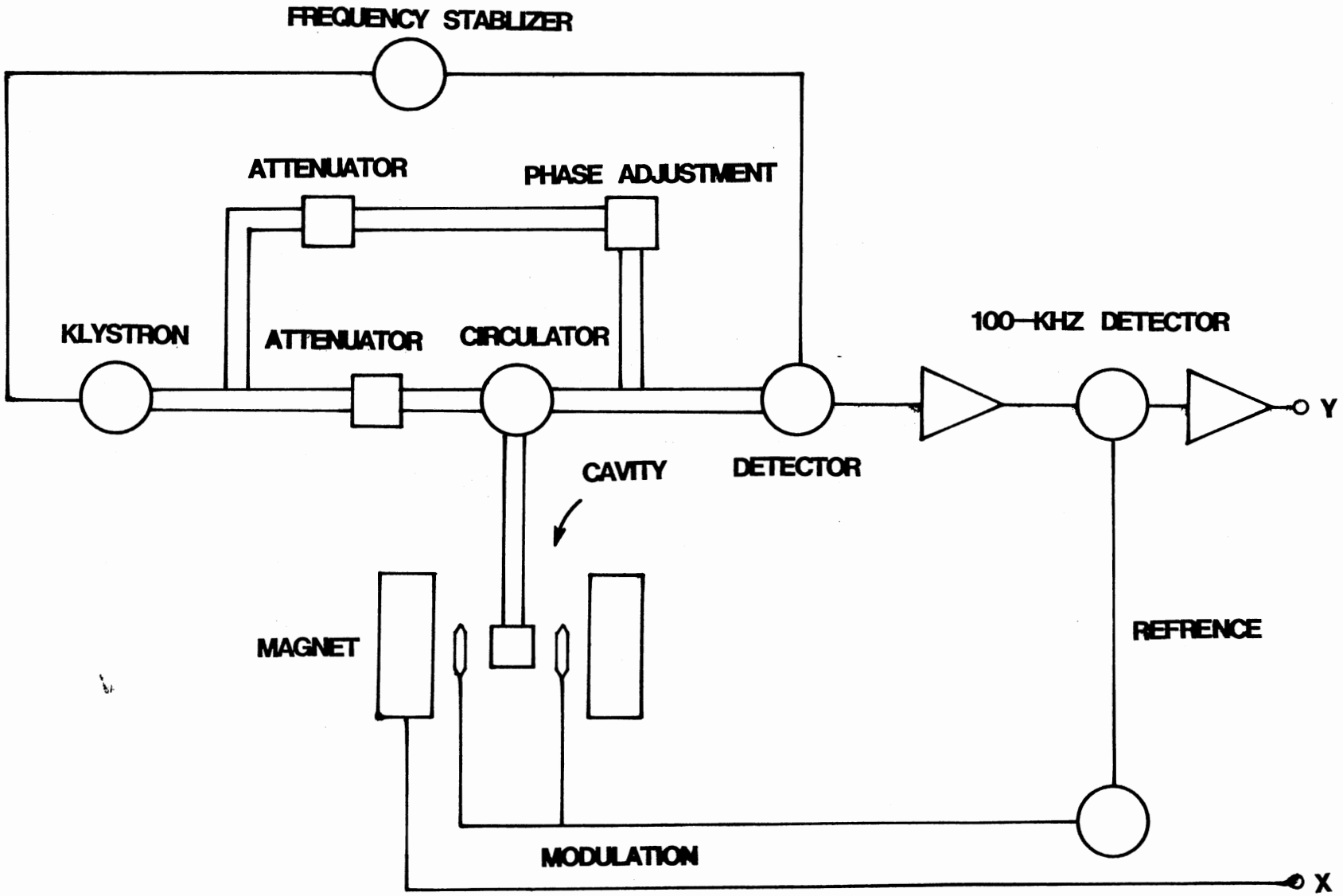

Figure 15. A Block Diagram of ESR Spectrometer

The $(AlO_4)^o$ center was monitored at 77 K. The ESR spectrum of the $(AlO_4)^o$ center is shown in figure 16. The $(AlO_4)^o$ center is formed by the substitution of Al^{3+} for Si^{4+} with a trapped hole for charge neutrality. The $(AlO_4)^o$ center can be produced by direct irradiation at room temperature or by irradiation at 77 K followed by the warming to room temperature.

The early suggestion of $(AlO_4)^o$ involvement in the production of the 110 C TL peak (14) was further tested. We examined the change in the $(AlO_4)^o$ concentration that occured following heating the sample to 150 C, from room temperature, and holding it at 150 C for 5 minutes. This temperature range corresponds to the range over which the TL signal appears. The sample had been irradiated for 1 minute using the Van de Graaff at room temperature. This change in $(AlO_4)^o$ concentration was then compared to the size of the TL peak. This experiment was done for each of the different kinds of samples. If the $(AlO_4)^o$ is responsible for 110 C TL peak, when the sample is heated to 150 C the decrease in $(AlO_4)^o$ concentration should, in some way, be related to the TL peak size. The higher the TL intensity, the larger should be the decrease.

If we included both the natural and the synthetic samples in this study, no clear correlation seemed to appear. We believe that this is because the TL is affected by many different kinds of inter-related defects. Since many different defects with varying concentrations are

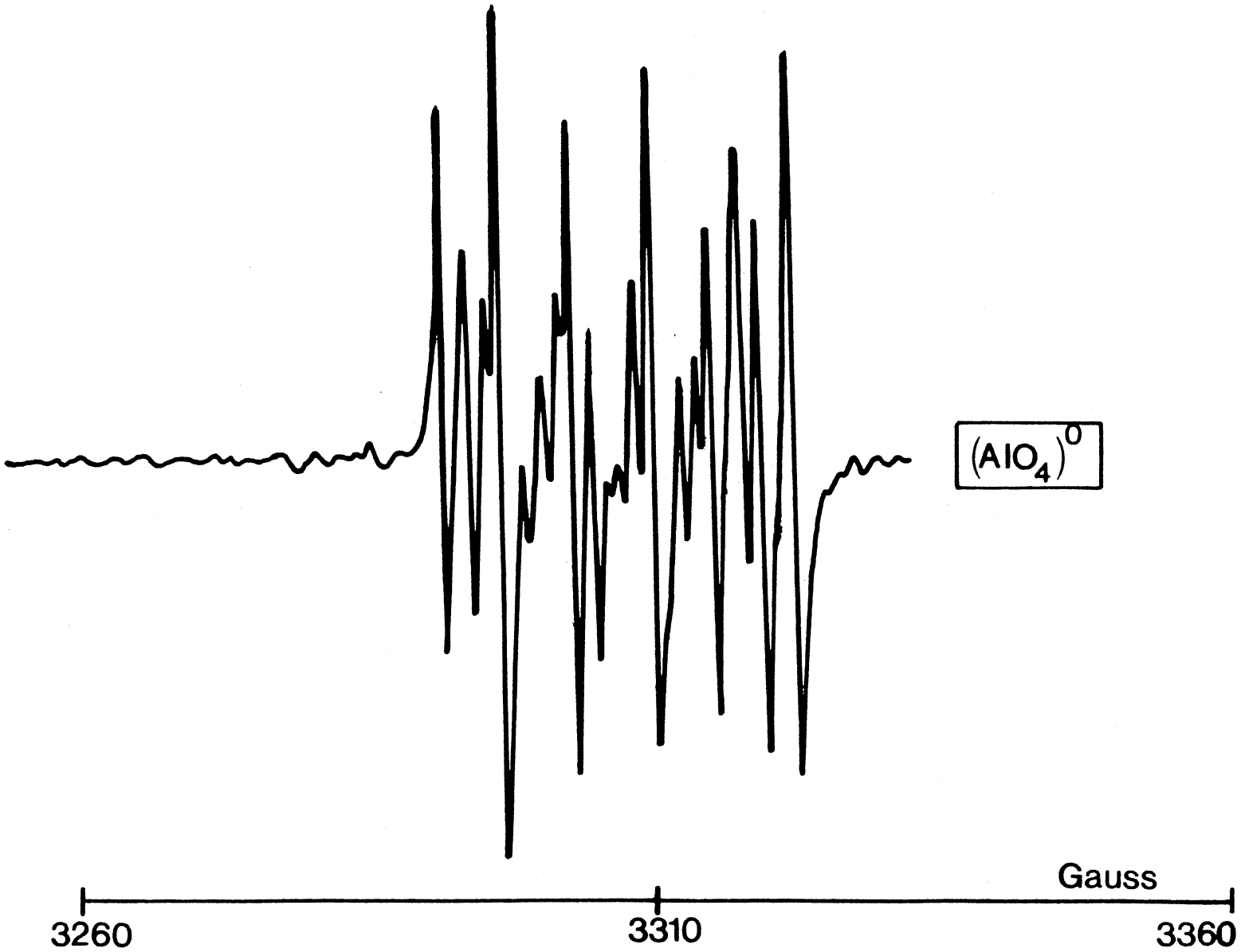

Figure 16. ESR Spectrum of the $(AlO_4)^0$ Center following One Minute Irradiation at Room Temperature Using the Van De Graaff Accelerator

present in natural samples, it is not too surprising that a clear correlation did not emerge.

However, if we choose the synthetic samples only, which have a similar defect structure, a much clearer picture appeared. Figure 17 shows a plot of TL peak height versus the decrease in the $(AlO_4)^o$ concentration for the synthetic samples. Both fired and as-received samples from X- and Z-growth regions were used. We can see that the decrease in the $(AlO_4)^o$ concentration is related to the TL intensity by a power law $TL \propto [(AlO_4)^o]^n$, with $n \doteq 1/2$. This result supports the suggestions that $(AlO_4)^o$ center is participating in the process of 110 C TL. One thing to be noted is that we do not expect a 1:1 correspondance in this case anyway since there is more than one recombination center.

A pulse annealing study was also made on the $(AlO_4)^o$ center. McKeever et al (14) have already showed that $(AlO_4)^o$ concentration decays around 110 C temperature region upon thermal annealing. In their case, however, the sample was irradiated at 77 K. Since the TL procedure for the Pre-Dose Effect usually involves irradiation at room temperature, it is worthwhile to repeat the annealing study with an irradiation at room temperature. As a representative, we plot the result for EZ samples in figure 18. Both fired and as-received samples were used. We can see that for both fired and unfired samples the curves decay around 100 C region. Comparing the behaviors of the two

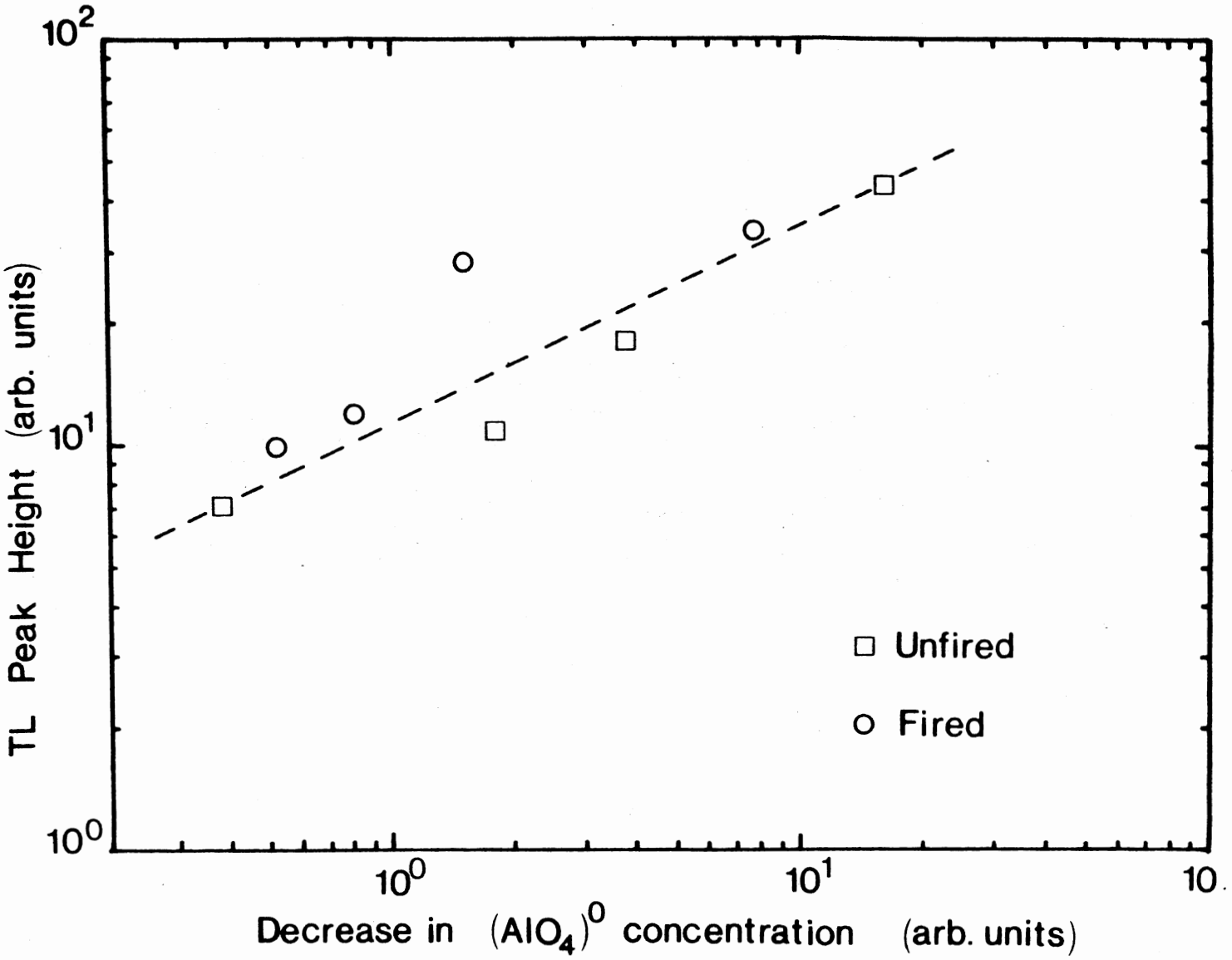

Figure 17. The TL Intensity of 110°C Peak versus the Decrease in the $(AlO_4)^0$ Center concentration During Heating to 150°C for Synthetic Samples

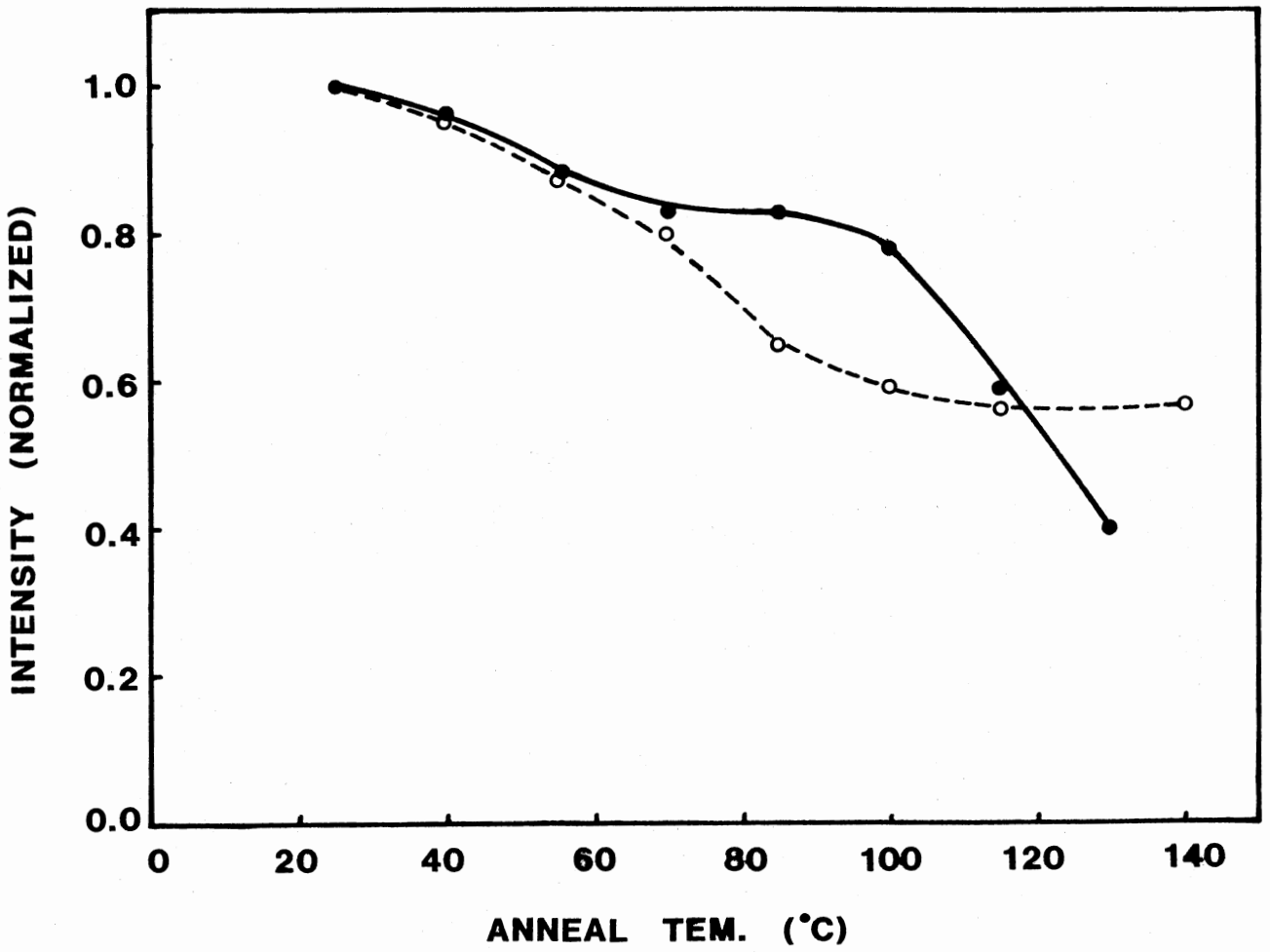

Figure 18. Pulse Annealing Study of $(AlO_4)^0$ Center Following a 6.6 Gy Gamma Irradiation at Room Temperature, the Circle Is for Fired EZ Sample while the Full Point Is for the As-received One

curves, an interesting feature is seen readily, i.e., the fired sample shows $(AlO_4)^o$ decay earlier (about 20 ^oC) than the unfired one. We relate this to the TL peak shift following firing of the sample, as described in the previous chapter. This follows naturally from the fact that for fired sample, the recombination happens earlier, resulting an early TL emission and an early decay of recombination center $(AlO_4)^o$. So this is another piece of supporting evidence that $(AlO_4)^o$ centers are involved in the production of the 110 ^oC TL peak.

The Ge-related Centers

Ge-related centers have been studied by Mackey (29) and others (30-31). The substitution of Ge^{4+} for Si^{4+} ion forms a class of defects related to the Ge^{4+} ion. When an electron is trapped in the vicinity of Ge^{4+}, it forms Ge(I) and Ge(II) centers. Here I and II stand for two different ways in which an electron can be trapped. The two centers are also called as $(GeO_4)^-$ and $(GeO_4)^-$ in the literature (32). When an interstitial alkali ion M^{+} is present, it forms $(GeO_4/M^+)^o$ centers. The ESR signals of the Ge-related centers are shown in figure 19.

After pulse annealing and an isothermal storage (at room temperature) study, McKeever et al (14) came up with the suggestion that the $(GeO_4)^-$ center is the electron trap for the 110 ^oC TL. They believe that the decrease of $(GeO_4)^-$ center over the 110 ^oC range has two reaction paths -- namely

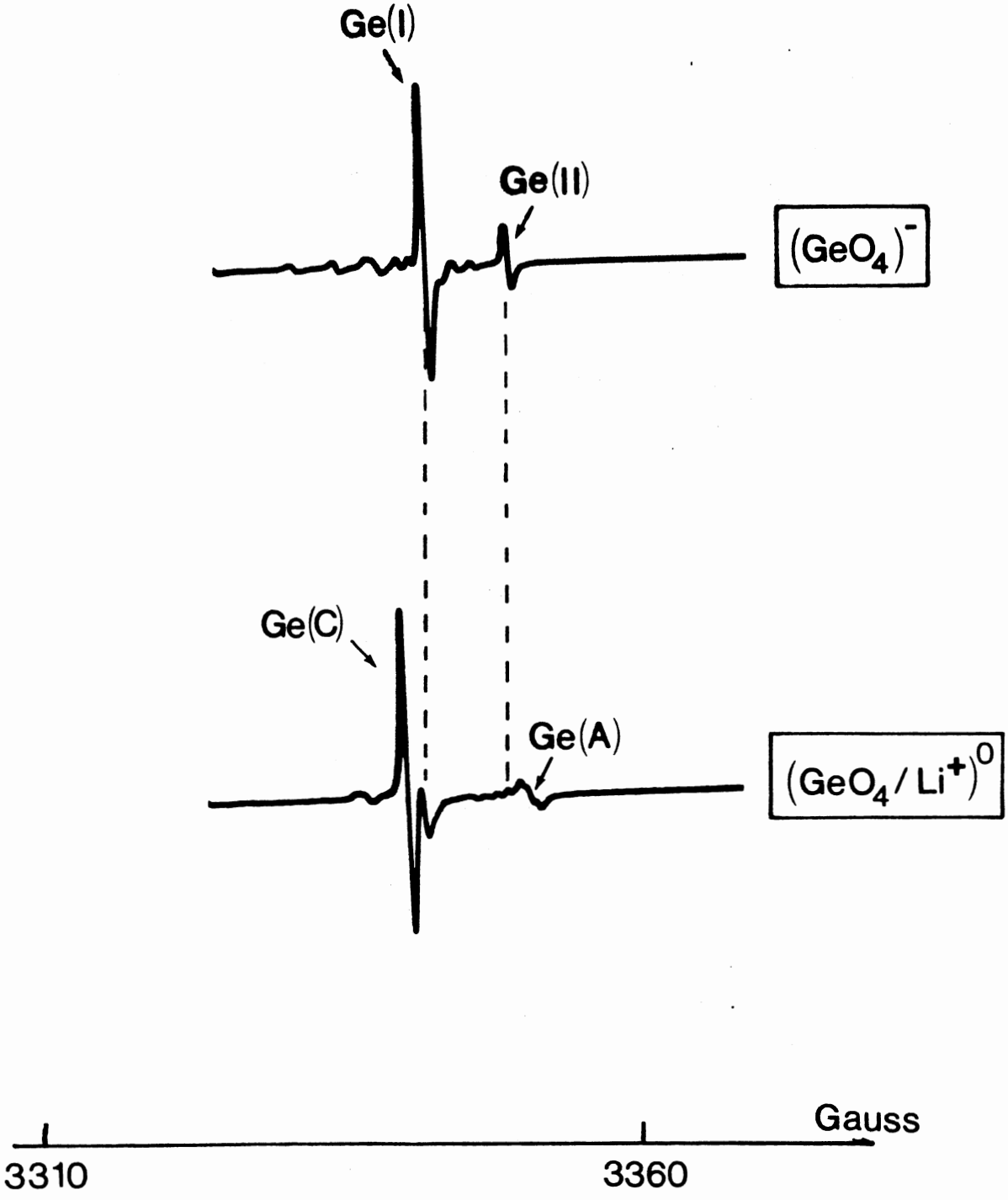

Figure 19. The ESR Spectrum of Ge-related Defects

the trapping of M^+ ions to form stable $(GeO_4/M^+)^o$ centers, or the loss of electrons to the recombination center (yielding TL). Again their study used an irradiation at 77 K. We use an irradiation at room temperature for the pulse annealing study to see if the curve follows a similar pattern.

Since the ratio of Ge(I) and Ge(II) is kept unchanged during the thermal treatment, we choose Ge(I) as a measure of Germaniun electron trap. Figure 20 is the plot of thermal behaviors of Ge(I) center and $(GeO_4/Li^+)^o$ center. The sample used here is the fired natural Arkansas quartz which has been given a gamma dose of 11 Gy at room temperature. The sample was held at the desired temperature for 2 minutes for the annealing. The centers intensities are normalized to their maxima. We see that irradiation at room temperature does produce $(GeO_4)^-$ centers. A small number of $(GeO_4/Li^+)^o$ centers is also present. After a few annealing steps, the $(GeO_4/Li^+)^o$ center reaches its maximum and several degrees later the Ge(I) center decays to a level almost invisible compared with the original value. For comparison, the decay of $(AlO_4)^o$ center is also plotted. We can see that both $(GeO_4)^-$ center and $(AlO_4)^o$ center decay in the same temperature range, although the decay happens earlier than the TL happens, probably due to the long annealing times. So the above experiment is consistent with the earlier suggestion of two reaction paths, one leading to TL.

Similarly, we have done the thermal annealing of the

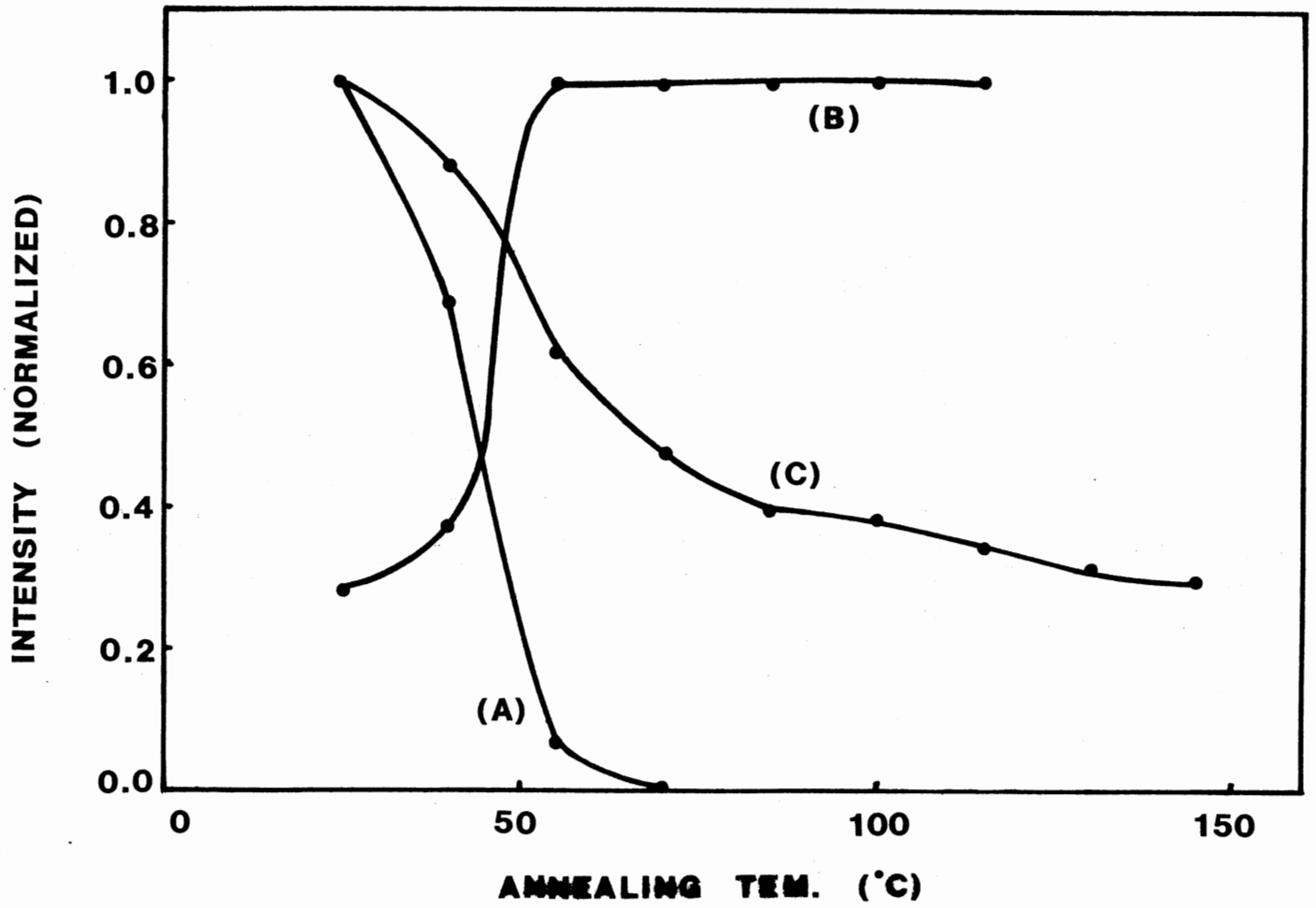

Figure 20. Thermal Behavior of Ge(I) Center (A) and $(GeO_4/Li^+)^0$ Center (B) for Arkansas Quartz, Also $(AlO_4)^0$ Center Is Represented by Curve (C)

$(GeO_4)^-$ center for both fired and unfired Arkansas sample, trying to see if the $(GeO_4)^-$ center decays earlier in the fired sample. But in contrast to the $(AlO_4)^o$ behavior, the $(GeO_4)^-$ decay for both fired and unfired samples seems follow the same step. Since $(GeO_4)^-$ center has two reaction paths, it is difficult to distinguish between that part of the decay which is due to the release of electrons to $(AlO_4)^o$ centers, from that part which is due to the trapping of Li^{4+} ions. It may be because of this combination that the $(GeO_4)^-$ center decays with the same step before and after firing. At this stage, further experiments are needed for verification.

$(H_3O_4)^o$ Center

In chapter I, we outlined the reaction paths for the 110 °C TL peak given by McKeever et al (14). The thermally released electrons recombine with two hole centers, of which the unknown center is believed to be responsible for the Pre-Dose Effect. In chapter II, we also suggested that hydrogen ions maybe play a very important role in the Pre-Dose Effect. Bearing this in mind in searching for the unidentified center, we suggest that the unknown center must have the following properties. (i) it must be a hole trap; (ii) it must be thermally unstable near 100 °C; (iii) it may be related to hydrogen.

One of the possible candidates for this unknown center is the $(H_3O_4)^o$ center. The $(H_3O_4)^o$ center was first

reported by Nuttall and Weil (33). This hole center is similar to the $(AlO_4)^o$ center. In this case, however, three protons occupy a silicon vacancy instead of an Al^{3+} ion. The ESR spectrum of the $(H_3O_4)^o$ center is shown in figure 21. This hole center was further studied by Chen (34). The thermal annealing curve given by him reveals that the $(H_3O_4)^o$ center decays significantly in the region of room temperature to 150 °C.

Both sets of authors used an irradiation at 77 K to produce the $(H_3O_4)^o$ center. The first thing we tested is to see if this center can be produced directly by irradiation at room temperature. The answer is positive. We subjected a PZ sample to an irradiation by electrons from the Van de Graaff accelerator at room temperature for 10 minutes. The $(H_3O_4)^o$ signal was subsequently observed at ~ 20 K.

We have made a thermal annealing study of the $(H_3O_4)^o$ center for both fired and as-received EX samples. The samples were irradiated for extended times (30 minutes) at 77 K. he annealing curves are shown in figure 22. We can see that for the fired sample, the $(H_3O_4)^o$ center decays faster than that for as-received sample. This feature is also present in the study of $(AlO_4)^o$ center. Indeed, the inset in figure 22 shows that after firing the $(AlO_4)^o$ and $(H_3O_4)^o$ centers decay in exactly the same way, suggesting the same annealing mechanism for both. Similarly, we can explain this by the argument that for fired sample the recombination happens earlier. Relating this to the peak

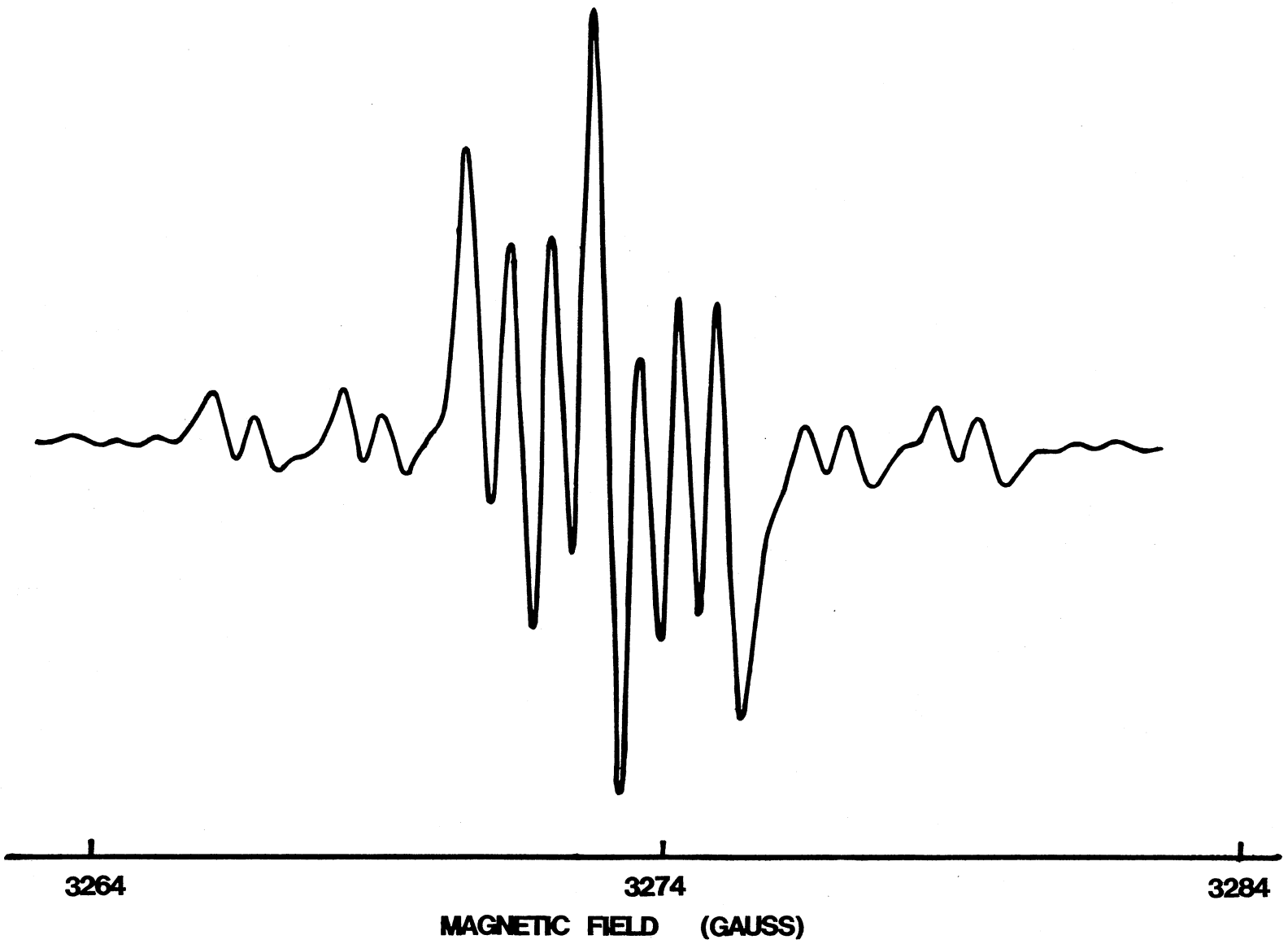

Figure 21. ESR Spectrum of the $(H_3O)^0$ Center

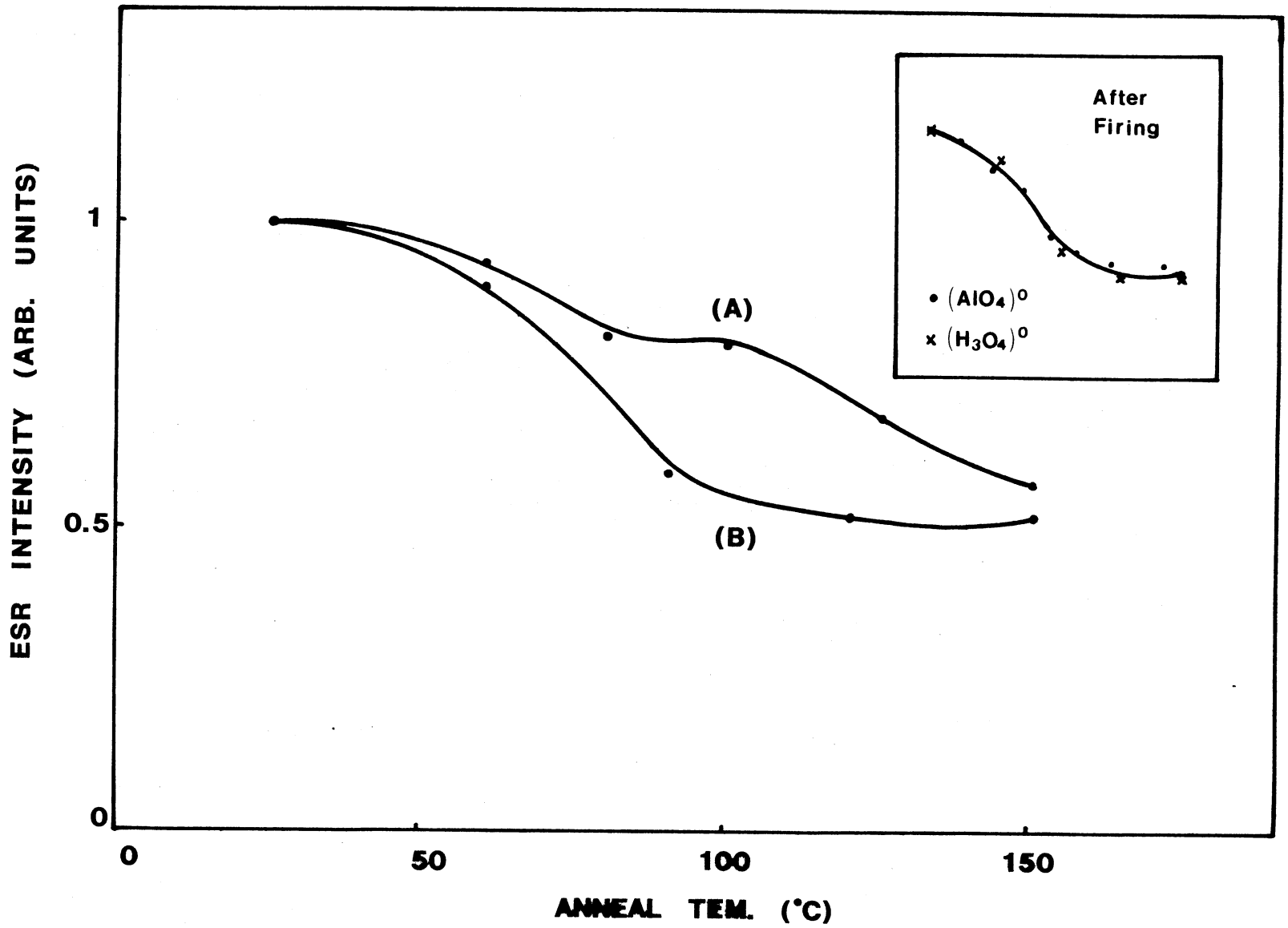

Figure 22. Thermal Behavior of the $(H_3O_4)^0$ Center, Curves (A),(B) Represent the As-received EX and Fired EX Samples, respectively

shift of TL following firing, we can see that $(H_3O_4)^o$ center is also involved in the TL production.

Another test is to see the involvement of $(H_3O_4)^o$ center in the Pre-Dose Effect. We use a similar procedure to that used in the activation of Pre-Dose Effect in TL. It is the following: (1) Irradiate the sample using the Van de Graaff for a total time of 10 minutes at room temperature in steps of 30 s, with 30 s intervals between steps (so that the sample is not heated up). (2) Cool the sample to about 20 K to monitor the $(H_3O_4)^o$. (3) Take the sample to a furnace and heat it to 400 C. Hold for 5 minutes. (4) Repeat the irradiation and ESR measurement.

In this procedure, we used a much bigger irradiation dose compared to that for TL. This is necessary for the easy detection of ESR. The first irradiation is supposed to be the "Pre-Dose". The sample used is a fired PZ. We choose PZ since it is supposed to have less Aluminum impurity and thus it is easier to monitor the $(H_3O_4)^o$ by ESR.

The result gives us a roughly 20 percent increase in the intensity of $(H_3O_4)^o$ center for the second measurement. The smallness of the increase compared to TL can also be explained by the same token, i.e., the sensitivity of ESR is smaller than that of TL and the 110 C TL peak can be greatly affected by the small changes in the defects. The important thing is that the $(H_3O_4)^o$ center does increase after the activation. Although the above procedure is not exactly the

one used for the thermal activation for TL, this is the closest we can get for the comparison between TL and ESR. The increase in $(H_3O_4)^o$ implies that the $(H_3O_4)^o$ centers do participate in the "Pre-Dose" phenomenon.

Another possible candidate of the unidentified hole center is the so-called "H-3" center (34). Although the origin of this center is not known yet, it is related to hydrogen. This also decays in the 100 ^oC temperature region. However, this center appears only after irradiation at 77 K. We tried to produce it by irradiation at room temperature and failed to do so. Since this center can not be produced by irradiation at room temperature, we rule out this center.

Effect of Firing

In chapter II, we have shown that the firing of the quartz samples greatly increases the TL sensitivity. Similarly, we examined the effect of firing on the strength of changes in the defect concentrations determined by ESR.

As described in chapter II, the E_1' center decreases by a factor about 4 following firing of the sample. The ESR spectrum of E_1' center is shown in figure 23. We follow Jani et al's suggestion (27) of E_1' production: i.e., an irradiation at room temperature followed by annealing at 300 ^oC. In our case, we gave the EX sample a 10 minutes electron irradiation, then annealed the sample at 300 ^oC for 15 minutes. The ESR was taken at room temperature.

For the $(AlO_4)^o$ center, the concentration increases (at

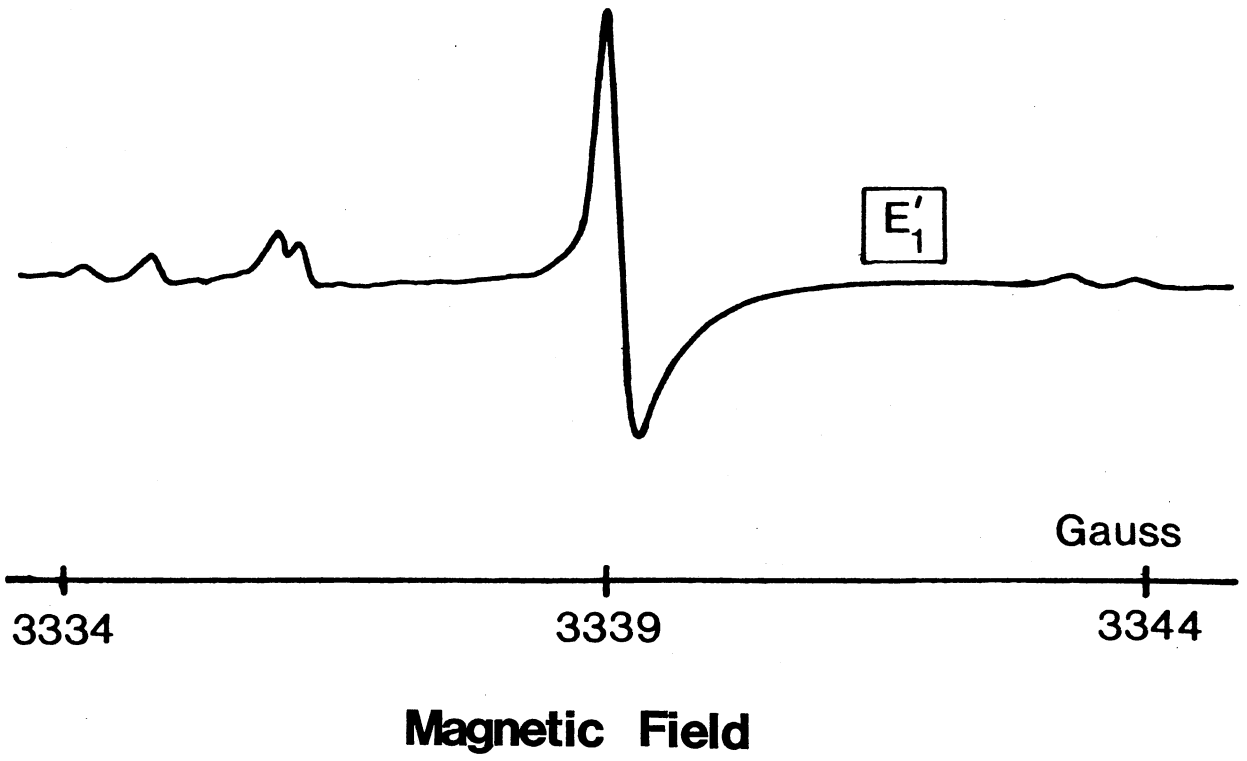

Figure 23. ESR Spectrum of E_1' Center

the most) by a factor of 2 after firing for PZ sample. For $(GeO_4)^{o}$ center, an even smaller increase is observed. All these defect variations following firing are very small compared with the corresponding TL change. However, the small change in defect concentrations might drastically change the TL intensity. One thing to be pointed out is that quantitatively these numbers maybe small but the changes do happen in the desired direction.

Summary

In this chapter, we presented ESR results which support the suggestion that the $(GeO_4)^{o}$ center, as well as the $(AlO_4)^{o}$ center are participating in the production of the 110 C TL peak. Based on the combined use of TL and ESR, we suggest that the $(H_3O_4)^{o}$ center is the "unknown" hole center which is responsible for the "Pre-Dose" Effect.

CHAPTER IV

INFRARED ABSORPTION

Based on the knowledge gained from TL and ESR, we suggested that hydrogen plays a very important part in the Pre-Dose Effect. In chapter III, we made a proposition that the $(H_3O_4)^o$ center is the recombination center responsible for the Pre-Dose Effect. In this chapter, we investigate the behavior of the near infrared absorption spectrum of quartz in the 3100 to 3700 cm^{-1} region. The absorption lines in this region represent O-H stretching vibrations. We can monitor the variation of these lines in response to the irradiation and thermal treatments. In this way, we hope to get more information on the role of hydrogen.

Experimental Detail

The samples used were both synthetic and natural material. Synthetic samples were cut into dimensions of 20 x 3 x 15 mm^3 in the X, Y and Z directions, respectively. The samples were taken mainly from the X-growth region and partly from the Z-growth region because of the size limitation of the samples. For the natural sample, the 3 mm side is along the Z direction.

Irradiations were performed using 1.7 MeV electrons from the Van de Graaff accelerator and were made at room

temperature using a metal Dewar with a 0.005" thick aluminum window in front of the sample. Since the penetration depth of these electrons is about 2 mm in SiO_2, to ensure uniform irradiation of the sample, we irradiated the sample on both sides with equal times. Again we used short pulses of irradiation to prevent heating of the sample.

The IR absorption data were obtained at 80 K from a Beckman 4240 spectrophotometer with approximately 5 cm^{-1} resolution. The spectrophotometer has dual beams produced from a Nernst globar source. The sample was placed in the Dewar mentioned above which, in turn, was placed on a holder provided by the Beckman 4240 so that the unpolarized incident light can propagate through the sample. The signal was detected by a thermocouple and recorded on an HP85 computer.

Thermal annealing was carried out in air in a tube furnace. Each time the sample was taken out of the dewar and heated at the desired temperature for 5 minutes.

Results and Discussion

IR Absorption for Synthetic Quartz

As representatives, two IR absorption spectra for the EG sample are shown in figure 24. Curve (A) is for the as-received sample. The four s-bands are the so-called "growth defects" which are OH-related defects of (as yet) unknown structure. Curve (B) in figure 24 is for the same sample irradiated at room temperature for one minute on each side.

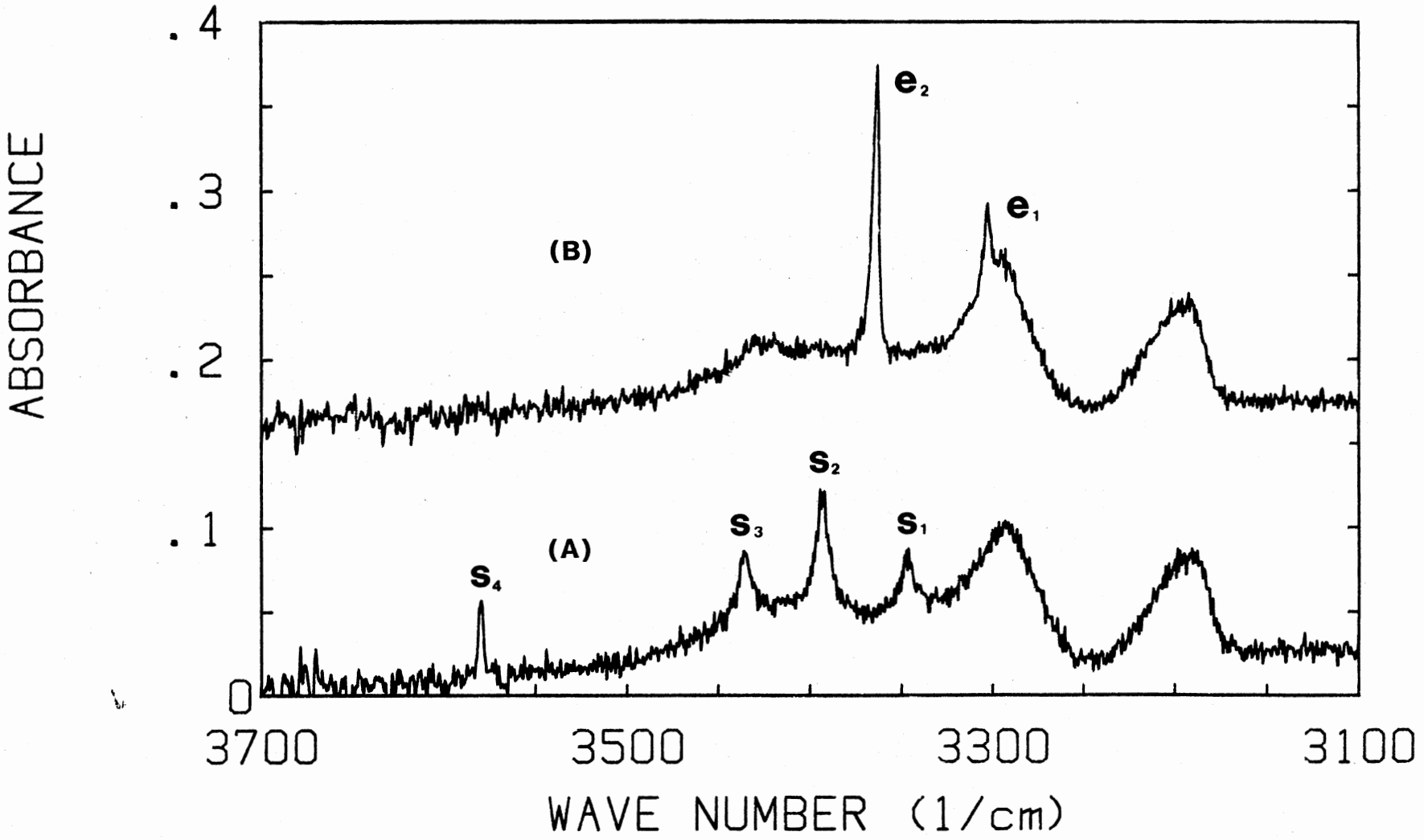

Figure 24. IR Absorption Spectra for the EG Sample, Curve (A) Is for the As-received Sample; Curve (B) Is for the Sample after Irradiation at Room Temperature

It can be seen that after irradiation the s-bands have diminished while two new bands (e_1 and e_2) have appeared. The structure responsible for the e-bands was suggested to be an OH^- molecule adjacent to a substitutional aluminum by Kats (35). The PQ sample has similar spectra but with a lower absorbance, probably due to the smaller impurity concentrations present.

Thermal annealing studies were made following irradiation of the sample at room temperature. In each case, the samples were given a sufficient irradiation dose to saturate the e-bands. Figure 25 shows the results for the PQ sample. Curve (A), (B) are for the as-received and fired samples, respectively. We can see that during the 300 °C-to-450 °C temperature region the e_2-band decays to zero while the s-band recovers. In this temperature region, the hydrogen ions move back from the Al-OH centers to the growth defects.

It is interesting to note that the Al-OH band increases in the temperature region from 200 °C to 300 °C. This probably means that hydrogen ions are released from other sources and move to the vicinity of Al. If we compare this with the TAC curve of the PX sample (fig. 13, curve (A)), we find that this is also the temperature region over which the TL sensitivity increases. This suggests a correlation between the movement of hydrogen and the increase in TL sensitivity during the Pre-Dose Effect. The enhancement of the TL maybe due to some hydrogen ions having moved into the precursor of

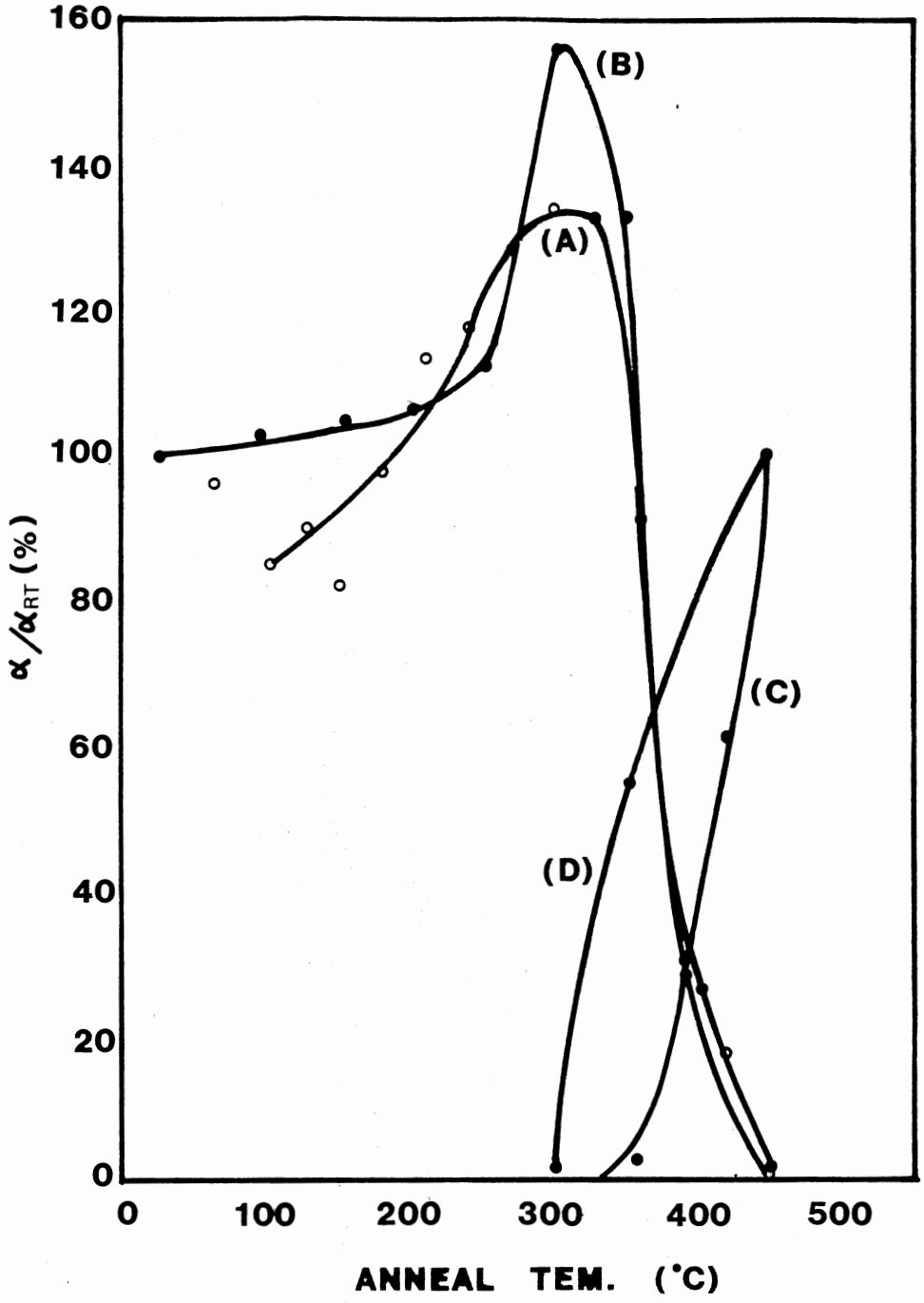

Figure 25. Thermal Annealing Behavior of the 3306 cm^{-1} Band, Curves (A),(B) Represent the Result for Unfired and Fired Samples, respectively, Also, the Recovery of the S Band for Unfired and Fired Quartz are Shown by Curves (C) and (D)

the recombination center ($(H_3O_4)^{o}$). Similar features can be observed for the EG sample. The results are shown in figure 26.

A similar thermal annealing study was done by Subramanian et al (36). In their case, however, the sample was irradiated at 80 K rather than at room temperature. Sibley et al (37) have observed a similar decay of the e-bands over the 300^{o}-to-450^{o} temperature region using an irradiation at room temperature. However, the increase in the e-band over the region of 200-300^{o} is very small in their case. Their procedure of annealing included a quenching of the sample in liquid nitrogen after being held at the desired temperature.

IR Absorption for Natural Quartz

The absorption spectrum for as-received natural Arkansas quartz is shown in figure 27. The spectrum consists of two big Al-OH bands and two relatively-small s-bands. The existence of Al-OH bands may be due to the natural irradiation received by the sample during its geological time. Another peak at 3475 cm^{-1}, which exists only in the natural sample, is also present. When the sample was irradiated at room temperature the Al-OH bands increased and the s-bands decreased.

A thermal annealing study was made after the (Al-OH) bands were saturated by irradiation at room temperature. Figure 28 gives the result. We found that the e_2-band

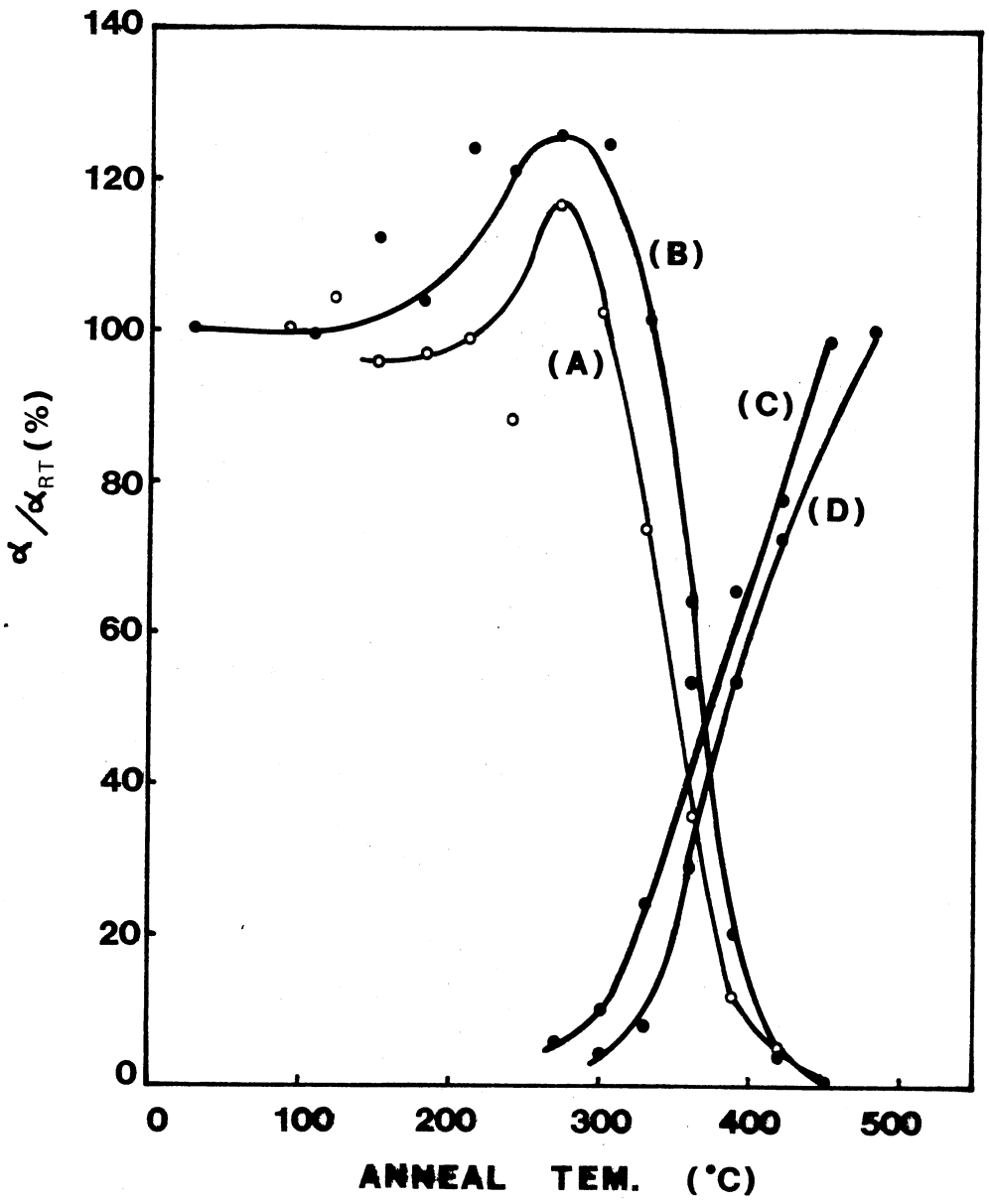

Figure 26. The Thermal Annealing Behavior of the 3306 cm^{-1} Band for EG Sample, Curves (A) and (B) Represent the Results for Unfired and Fired Samples, Respectively, Also, the Recovery of S Band is Shown by the Curves (C) and (D)

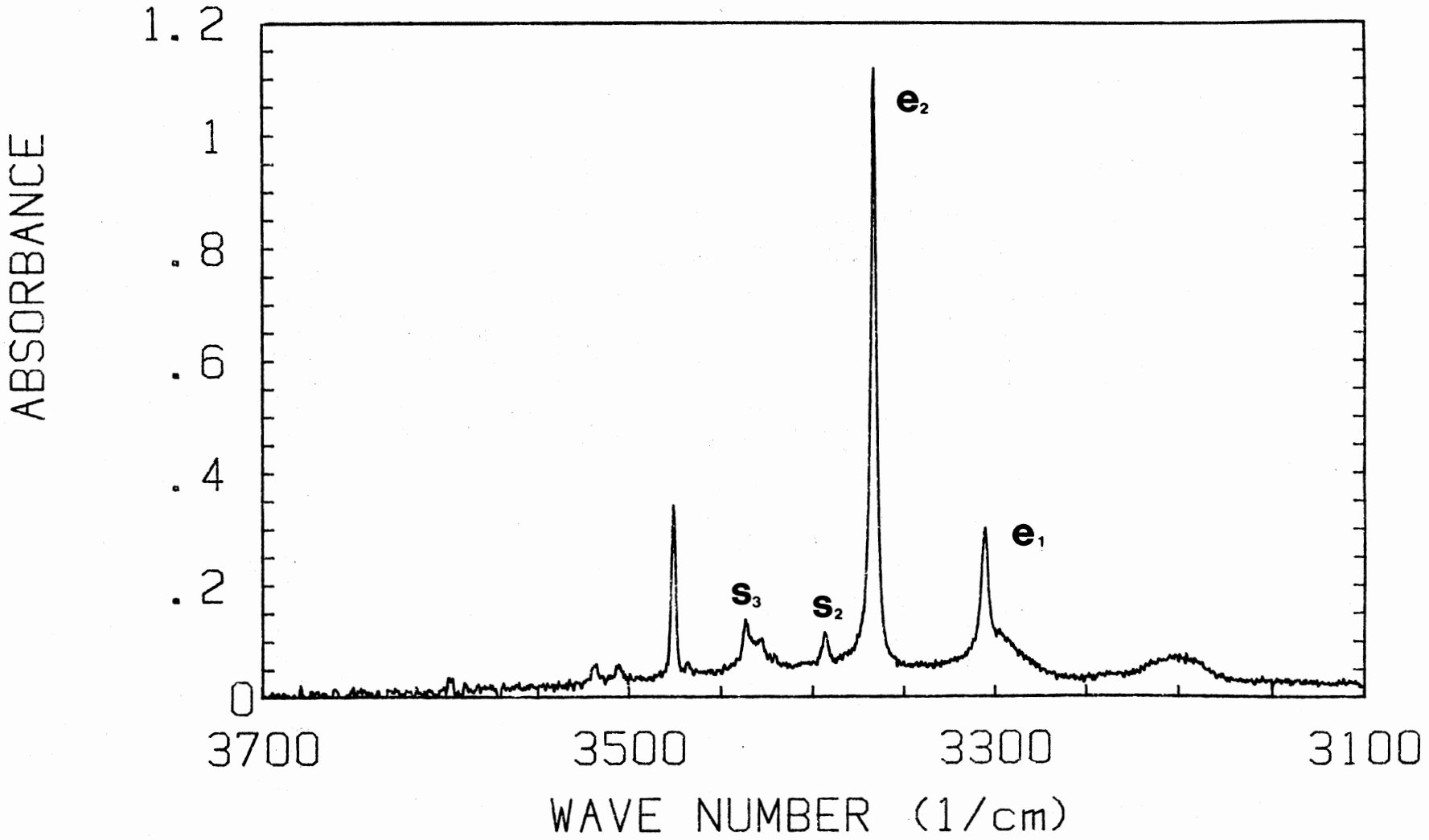

Figure 27. IR Absorption Spectrum for Natural Arkansas Quartz

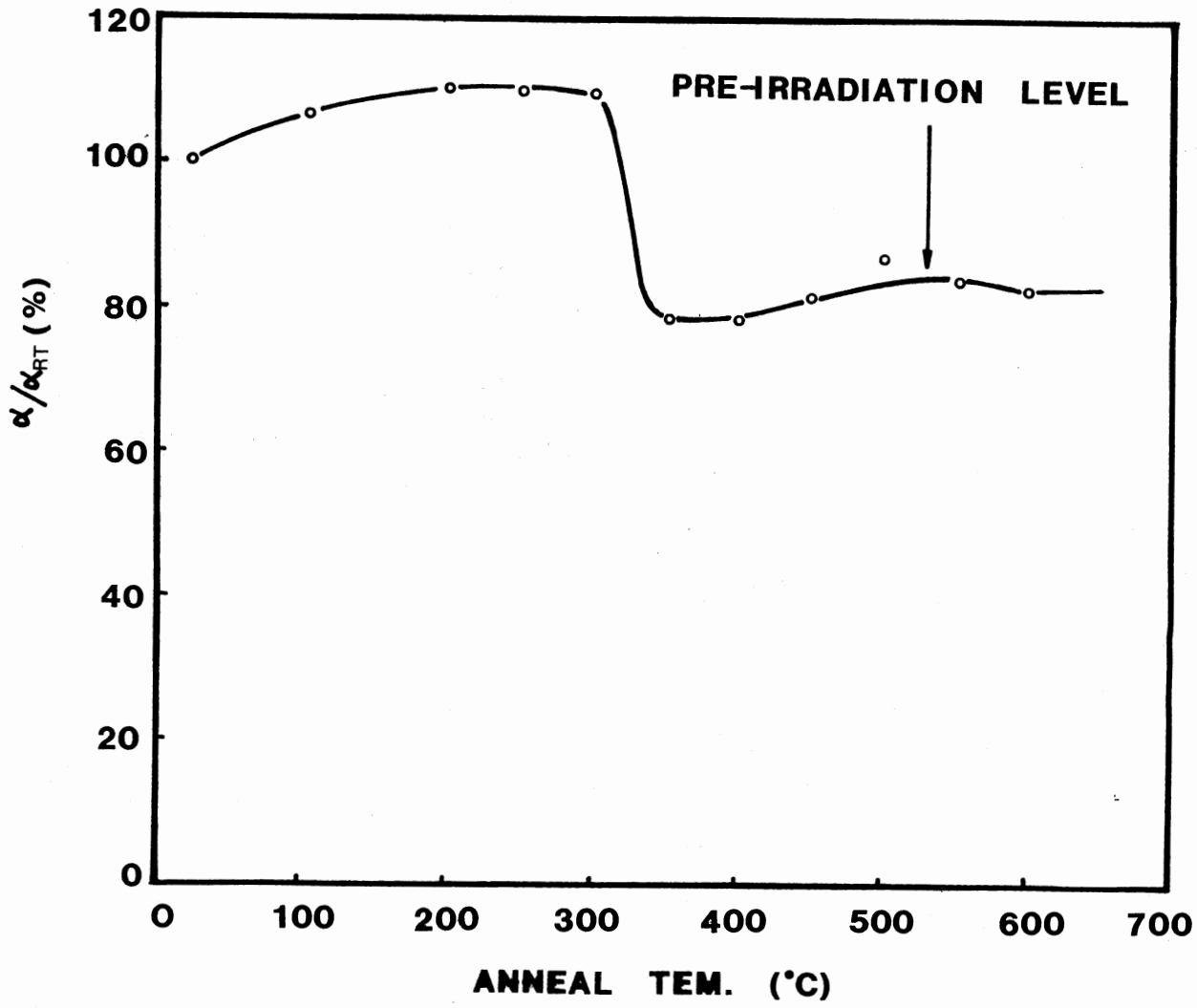

Figure 28. The Annealing Behavior of e_2 Band in Arkansas Quartz

decreases around 300 °C and then becomes stable at the level before irradiation, until 600 °C. If we just consider the change in that part of e_2 which is induced by irradiation, we find that it decays to zero by 350 °C. Although for a sample without irradiation the e-bands did not decay until after 600 °C, for an irradiated sample, however, the e-band does decay and the s-bands come back. Once again the study reveals that the hydrogen ions move around in the lattice in the temperature region over which the TL sensitivity starts to increase (figure 13, curve (C)). Differing from synthetic sample, however, an obvious correlation between TL and hydrogen ion movement is lacking for natural sample, this is probably due to the fact that the situation in natural samples is much more complicated and the hydrogen movement can not be revealed by just monitoring OH bands.

Summary

In this chapter, by monitoring the thermal behavior of Al-OH bands, we can see that a correlation exists in synthetic quartz between the activation of the Pre-Dose Effect and the movement of hydrogen. This is another piece of supporting evidence that hydrogen ions are involved in the Pre-Dose Effect and this is also consistent with the proposition of $(H_3O_4)^{\circ}$ centers act as the recombination centers. For natural quartz, however, a satisfactory explanation is lacking although the H ions move around near the 300 °C region.

CHAPTER V

SUMMARY AND CONCLUSION

In this thesis, we continued the study of the Pre-Dose Effect in crystalline quartz by examining the possible point defects involved in the production of the 110 °C TL peak. The emission spectrum of 110 °C TL peak consists of two broad peaks, predominantly at 380 nm with a weaker emission at ~ 470 nm. (3). It has been shown that the emission at 470 nm is caused by the recombination of electrons at $(AlO_4)^o$ centers (20). McKeever et al (14) verified that the Pre-Dose Effect itself is not related to the electron traps nor related to the $(AlO_4)^o$ centers. They predicted that the Pre-Dose Effect is due to the activation of the recombination centers which are responsible for the 380 nm emission. Later, Prescott (38) confirmed that the 470 nm emission did not increase by Pre-Dose activation while the 380 nm component was greatly enhanced by the Pre-Dose activation.

Based on the experimental results obtained from TL, ESR and IR, we suggest that the TL peak at 110 °C is produced by the recombinations of electrons released from $(GeO_4)^-$ centers with the two hole centers, namely, $(AlO_4)^o$ and $(H_3O_4)^o$. We suggest that the 380 nm emission results from the recombination of these electrons with holes at $(H_3O_4)^o$

centers. Pre-Dose activation "activates" the $(H_3O_4)^o$ centers. The involvement of H^+ ions is supported by the IR measurements which reveal that H^+ ions are mobile during Pre-Dose activation. The activation process could then be achieved by the trapping of H^+ ions at the precusors to the $(H_3O_4)^o$ centers, although a detailed knowledge of this process is still lacking.

It should be noted that the Pre-Dose Effect requires both irradiation and heating (3). The H^+ ion movement that we are observing occurs only after the sample has been first irradiated, and then heated. It appears that the irradiation "unlocks" the H from the "growth defects" and heating causes these H^+ ions to move.

The superlinear dose dependence of the TL sensitivity for the unfired samples was explained using a competition-during-heating model. The introduction of competitors during the heating stage of the TL process removes a flaw in Zimmerman's Model (5). Firing the sample removes the competitors so that for the fired sample the dose dependence is nearly linear and the TL sensitivity is high.

Based on the above information, we propose the following mechanisms for the Pre-Dose activation of quartz, described by the schematic TAC curve shown in figure 29. The thermal activation curve of an as-received sample is represented by curve (a). The increase in sensitivity, Δ_1, is due both to the removal of competitors and to the Pre-Dose activation of the $(H_3O_4)^o$ recombination centers. After

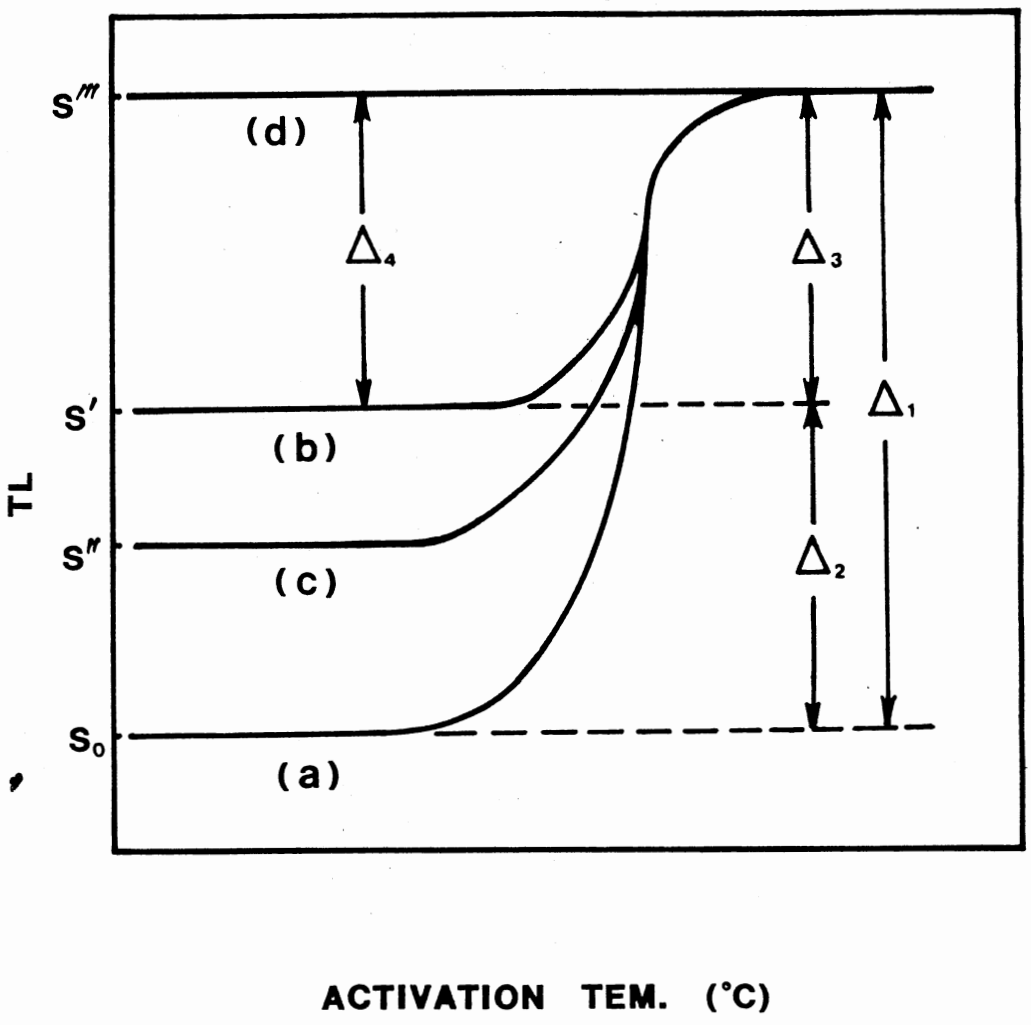

Figure 29. Idealised TAC Curves
Curve (a) Is for an As-received Sample
Curve (b) Is for a Sample Fired at 950 °C
Curve (c) Is for a Sample Fired Below 950 °C
And Curve (d) Is for a Swept and Fired Sample

a sample has been fired at 950 °C, the competitors have been removed so that the initial sensitivity S' goes up and the activation is now caused by the activation of the recombination centers only. The change Δ_3 is due to the Pre-Dose Effect only and Δ_2 is the increase in sensitivity due to the removal of competitors. Curve (c) shows the TAC for a partially fired sample, i.e., one fired to an intermediate temperature. In this case, the initial sensitivity S" will be between the values of S' and S_0. As the initial sensitivity increases, Δ_3, the increase due to the thermal activation, decreases. This gives the apparent anti-correlation between the initial sensitivity and the Pre-Dose Effect noted earlier (18). Sweeping affects the recombination centers. For a swept and fired sample, the competitors have been removed and the recombination centers have been saturated by the ion exchange so that the initial sensitivity S''' is high and further activation treatments have no effect on the sensitivity, i.e., there is no Pre-Dose Effect. This agrees with experimental observation (18). This situation is represented by curve (d). Δ_4 is the increase due to the ion exchange and clearly $\Delta_4 = \Delta_3$.

Further studies of Pre-Dose Effect should consist of an experimental test of the prediction sketched in figure 29. Also, since we say that sweeping saturates Pre-Dose Effect and that Pre-Dose Effect is due to an increase of $(H_3O_4)^o$, an ESR study can be made to directly check if the $(H_3O_4)^o$ concentration becomes bigger after sweeping. The search for

the competitors is still before us.

REFERENCES

1. Fleming, S. J., Pact 3, 325 (1978).

2. Fleming, S. J., Archaeometry 15, 13 (1973).

3. Zimmerman, J., J. phys. C: Sol. St. 4, 3265 (1971).

4. Fleming, S. J., D. Phil. Thesis, Oxford University. (1969).

5. Chen, R., Pact 3, 325 (1979).

6. David, M. et al, Ind. J. Pure Appl. Phys. 15, 277 (1977).

7. David, M., Ind. J. Pure Appl. Phys. 19, 1048 (1981).

8. McKeever, S. W. S., Radiat. Protect. Dosim. 8, 81 (1984).

9. McKeever, S. W. S., et al, Pact. 9, 123 (1983).

10. Aitken, M. J. and Fleming, S. J., Topics in Radiation Dosimetry Suppl. 1, 2 (1972).

11. Aitken, M. J., Pact 3, 319 (1979).

12. Aitken, M. J. and Murray, A. S., The 1976 symposium on Archaeometry and Archaeological prospection, Edingurgh, (ed. H. McKerrel). HMSO, London.

13. Halliburton, L. E., Cryst. Latt, Def. and Amorph. Mat. 12, 163 (1985).

14. McKeever, S. W. S. et al, Nucl. Tracks and Radiat. Meas. 10, 489 (1985).

15. Durrani, S. A., Groom, P. J., Khazal, K. A. R. and McKeever, S. W. S., J. Phys. D. Appl. Phys. 10, 1351 (1977).

16. O'Brien, M. C., Proc. R. Soc. A231, 405 (1955).

17. Mackey, J. H., J. Chem. Phys. 7, 220 (1963).

18. Martini, M., Spinolo, G. and Vedda, A. J. Appl. Phys.

61, 7 (1987).

19. Martini, M., Spinolo, G. and Vedda, A., Journal of luminescence . North Holland, Amsterdam, 40&41, 347 (1988).

20. Jani, M. G., Halliburton, L. E., and Kohnke, E. E., J. Appl. Phys. 54, 6321 (1983).

21. Ichikawa, Y., Japan J. Appl. Phys. 7, 220 (1968).

22. Aitken, M. J., Thermoluminescence dating (New York, Academic) P. 359.

23. Rodine, E. T. and Land, P. L., Phys. Rev. B4, 2701 (1971).

24. Kristianpoller, N., Chen, R. and Israeli, M., J. Phys. D. Appl. Phys. 7, 1063 (1974).

25. Chen, R. and Kirsh, Y., Analysis of thermally stimulated processes (Oxford Pergamon) P. 361.

26. Mondragon, M. A., Chen, C. Y. and Halliburton, L. E., J. Appl. Phys. 63, 4937 (1988).

27. Jani, M. G., Bossoli, R. B., and Halliburton, L. E., Phys. Rev. B27, 2285 (1983).

28. Martini, M., Sibilia, E., Spinolo, G., and Vedda, A., Nucl. Tracks. 10, 497 (1985).

29. Mackey, J. H. Jr., The J. Chem. Phys. 39, 74 (1963).

30. Anderson, J. H. and Weil, J. A., J. Chem. Phys. 31, 427 (1959).

31. Weil, J. A., Morris, A. H. and Anderson, J. H., Bull. Am. Phys. Soc. 4, 417 (1959).

32. Weil, J. A., Phys, Chem. Minerals. 10, 149 (1984).

33. Nuttall, R. H.D. and Weil, J. A., Solid state communications. 33, 99 (1980).

34. Chen, C. Y., Ph. D. Thesis, Oklahoma State University (1985).

35. Kats, A, Philips, Res. Rep. 17, 133 (1962).

36. Subramanian, B., Hallibarton, L. E. and Martin, J. J., J. Phys. Chem. Solids, 45, 575 (1984).

37. Sibley, W. A., Martin, J. J. Wintersgill, M. C. and

Brown, J. D., J. Appl. Phys., 50, 5449 (1978).

38. Prescott, J. R., Nucl. Tracks Radiat. Meas. 14, 21 (1988).

VITA

XIAO-HUA YANG

Candidate for the Degree of

Master of Science

Thesis: PRE-DOSE EFFECT AND POSSIBLY-RELATED POINT DEFECTS IN CRYSTALLINE QUARTZ

Major Field: Physiscs

Biographical:

Personal Data: Born in Zhengzhou, China, May 17, 1962, the son of Han Qing Yang and Yu Qing Gao.

Education: Graduated from eighth high school (Zheng Zhou, China) in 1980, received Bachelor of Science Degree in physics from Xinxiang Normal University in 1984; completed the requirements for the master of science degree at Oklahoma State University in December, 1988.